Artifact Reduction

Basic Short Course

Marc Kachelrieß

German Cancer Research Center (DKFZ)
Heidelberg, Germany
www.dkfz.de/ct

DEUTSCHES KREBSFORSCHUNGSZENTRUM IN DER HELMHOLTZ-GEMEINSCHAFT

This Presentation …

- discusses pragmatic and efficient approaches to reduce artifacts, such as
  - beam hardening artifacts,
  - cone-beam artifacts,
  - scatter artifacts,
  - metal artifacts, …
- does not discuss iterative reconstruction techniques that may be less susceptible to artifacts due to improved modeling
- does not discuss artifact avoidance techniques such as
  - special trajectories (to avoid cone-beam artifacts),
  - flying focal spot (to reduce sampling artifacts),
  - spectral shaping (to reduce beam hardening),
  - anti scatter grids or the iPMSE technique (to reduce scatter artifact),
  - beta blockers (to reduce motion artifacts), …

Artifact List

- glow artifacts
- Aliasing artifacts
- Beam hardening artifacts
- Blooming artifacts
- Calibration artifacts
- Cone-beam artifacts
- Correction artifacts
- Cross-talk artifacts
- Cupping and capping artifacts
- Defect detector pixel artifacts
- Display artifacts
- Electronic noise artifacts
- Ghost artifacts
- Limited angle artifacts
- Linear partial volume artifacts
- Metal artifacts
- Misalignment artifacts
- Missing data artifacts
- Motion artifacts
- Non-linear partial volume aritifacts
- Photon starvation artifacts
- Quantum noise artifacts
- Ring artifacts
- Sampling artifacts
- Scatter artifacts
- Streak artifacts
- Truncation artifa
- Windmill a

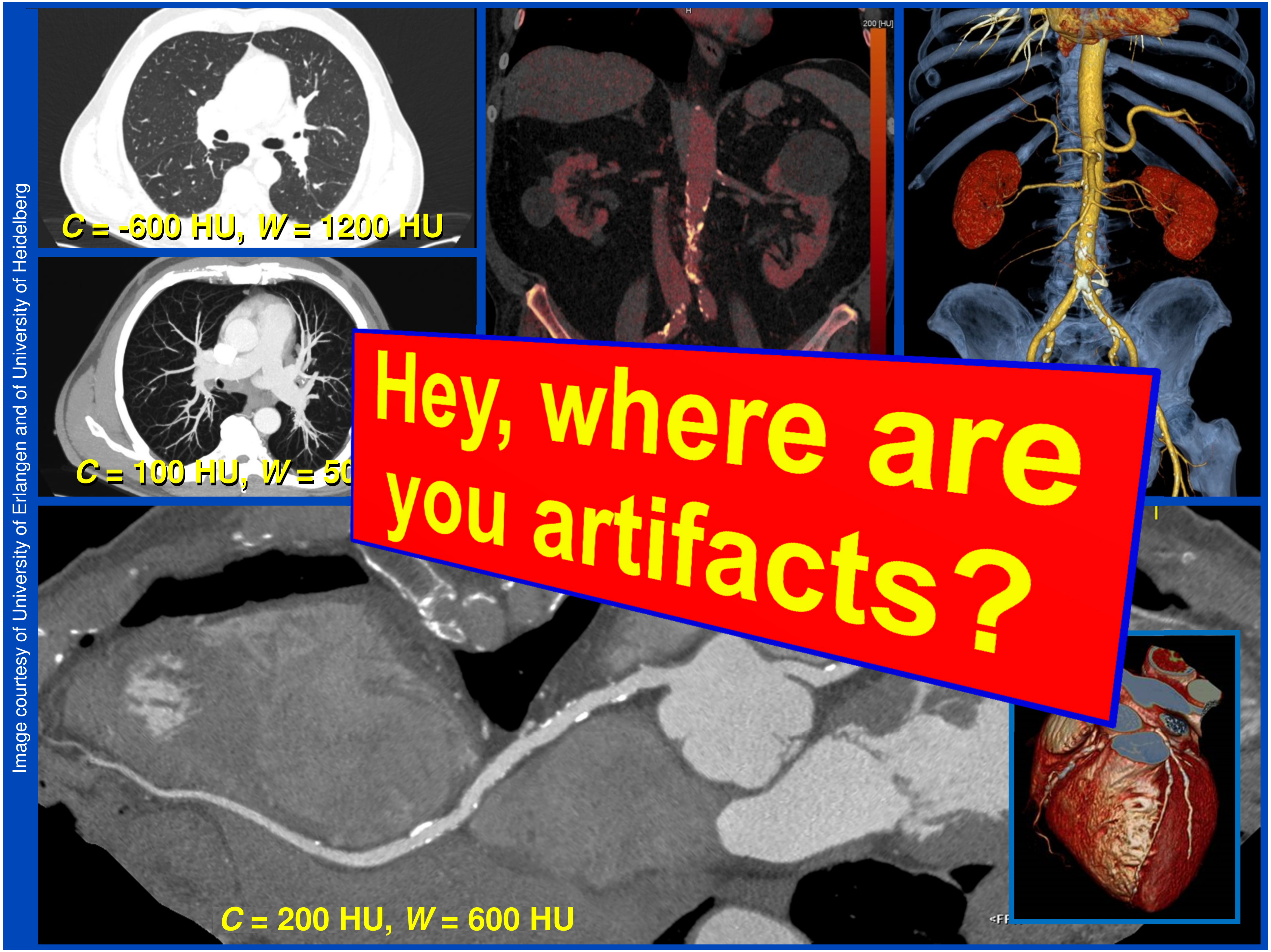

Image courtesy of University of Erlangen and of University of Heidelberg
C = -600 HU, W = 1200 HU
C = 100 HU, W = 50
Hey, where are you artifacts?
C = 200 HU, W = 600 HU

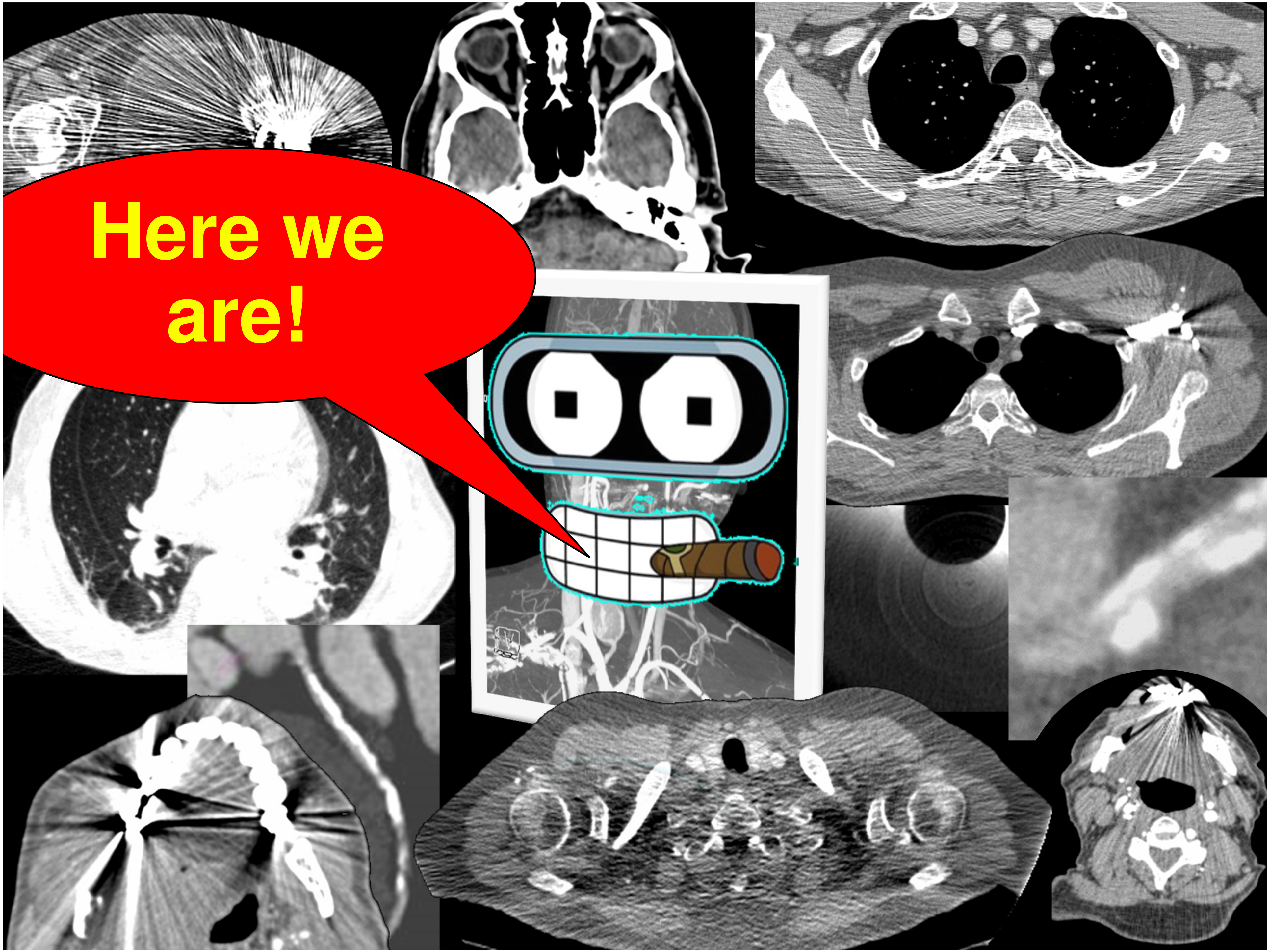
Here we are!

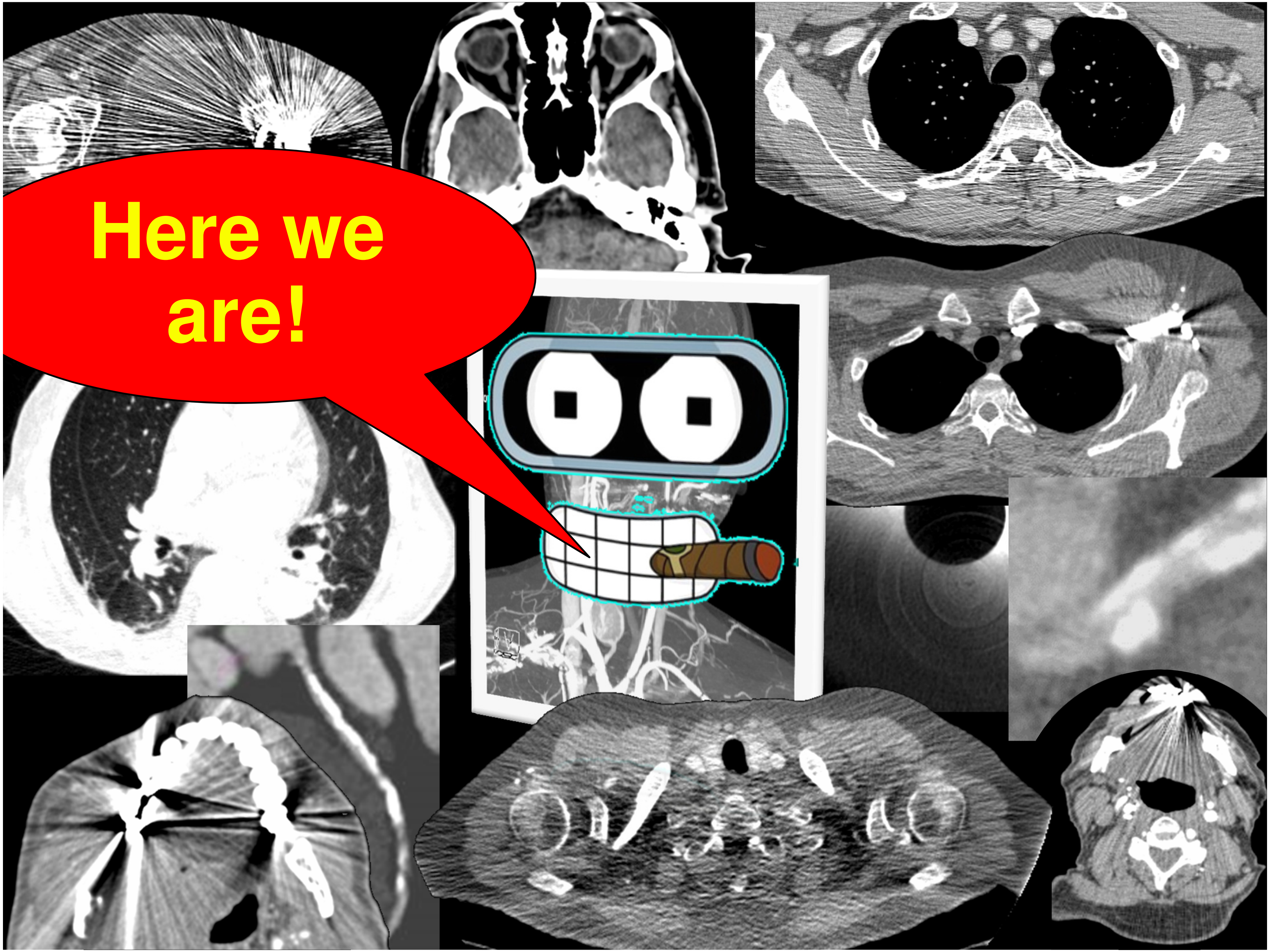
Here we are!

More or Less Artifacts?

- Less artifacts due to
  - new clinical CT detectors with extremely low electronic noise
  - better x-ray tubes and spectral shaping in clinical CT
  - improved anti-scatter grids in clinical CT
  - shorter rotation times in clinical CT
  - smaller detector pixels
  - …
- More artifacts due to
  - more applications in flat detector CT
  - low x-ray power in flat detector CT
  - less efficient anti-scatter grids in flat detector CT
  - long rotation times in flat detector CT
  - flat detetors with significant flaws: afterglow, electronic noise, low absorption efficiency, low stability, low dynamic range, …

GE Revolution CT

Philips IQon Spectral CT

Siemens Somatom Force

Toshiba Aquilion ONE Vision

In-plane resolution: 0.4 … 0.7 mm

Nominal slice thickness: S = 0.5 … 1.5 mm

Tube (max. values): 120 kW, 150 kV, 1300 mA

Effective tube current: mAs_{eff} = 10 mAs … 1000 mAs

Rotation time: T_{rot} = 0.25 … 0.5 s

Simultaneously acquired slices: M = 16 … 320

Table increment per rotation: d = 1 … 183 mm

Scan speed: up to 73 cm/s

Temporal resolution: 50 … 250 ms

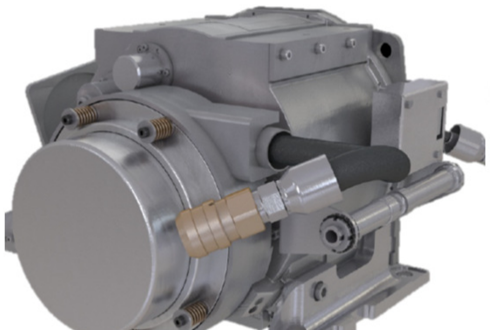

GE Performix HDw

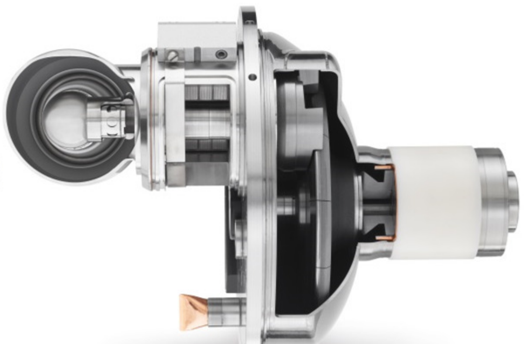

Philips iMRC

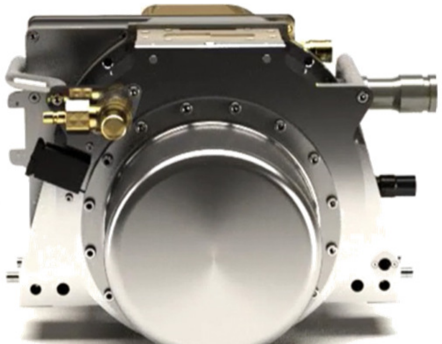

Siemens Vectron

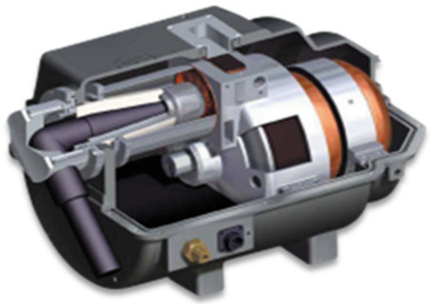

Toshiba Megacool Vi

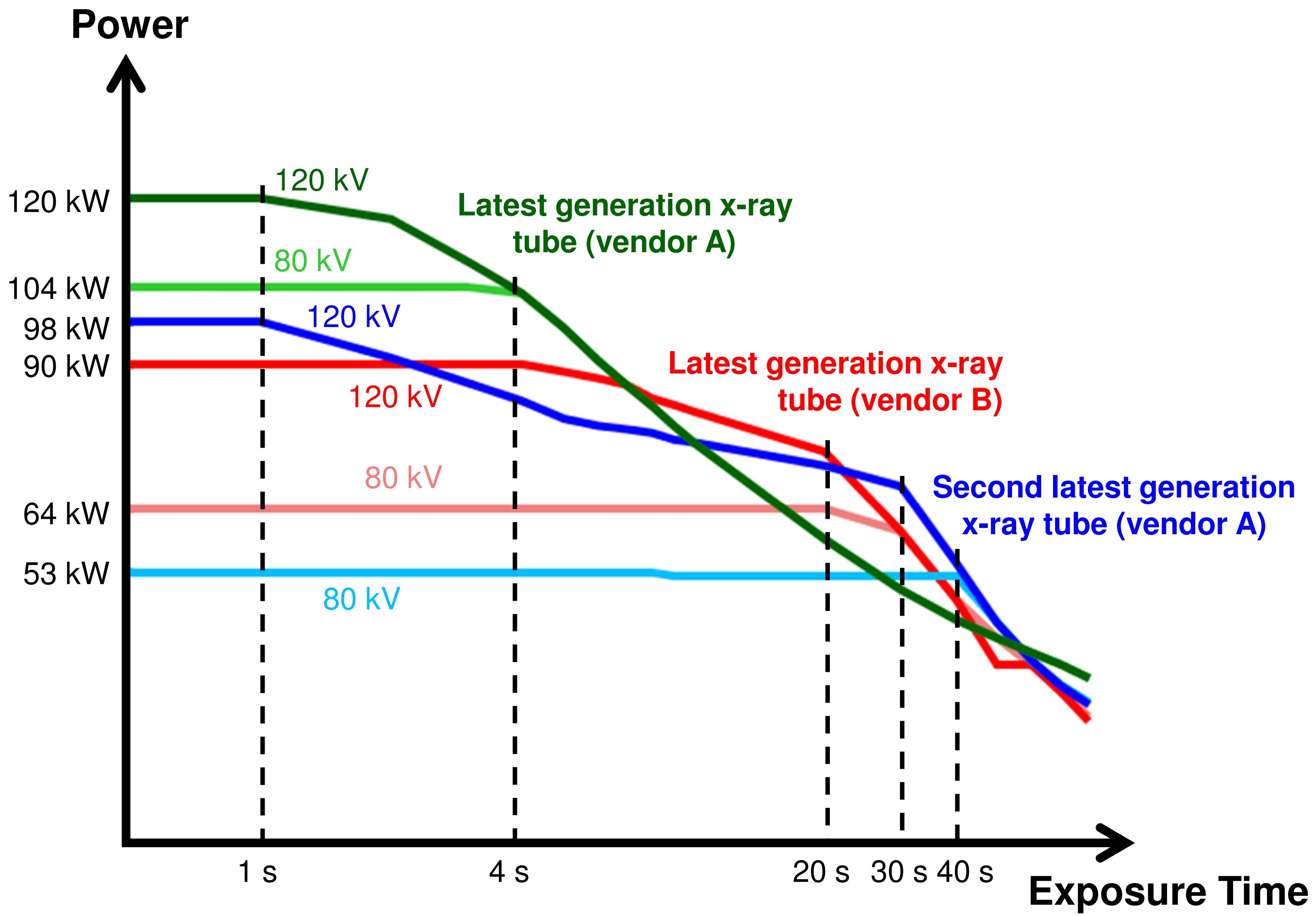
Power
120 kW
104 kW
98 kW
90 kW
64 kW
53 kW
120 kV
80 kV
120 kV
120 kV
80 kV
80 kV
Latest generation x-ray tube (vendor A)
Latest generation x-ray tube (vendor B)
Second latest generation x-ray tube (vendor A)
1 s
4 s
20 s
30 s
40 s
Exposure Time

120 kV + 0 mm water with and without prefilter

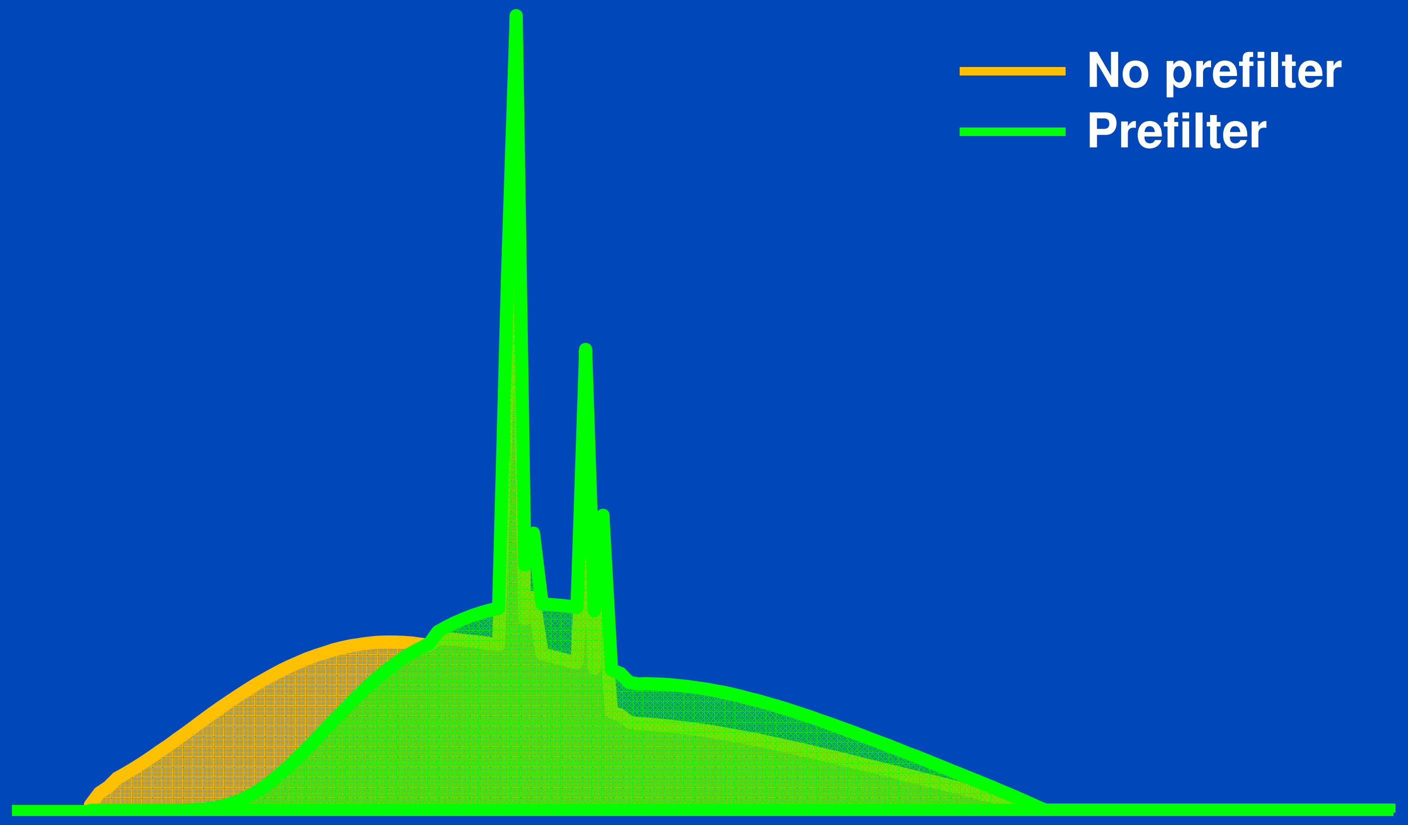

120 kV + 320 mm water with and without prefilter

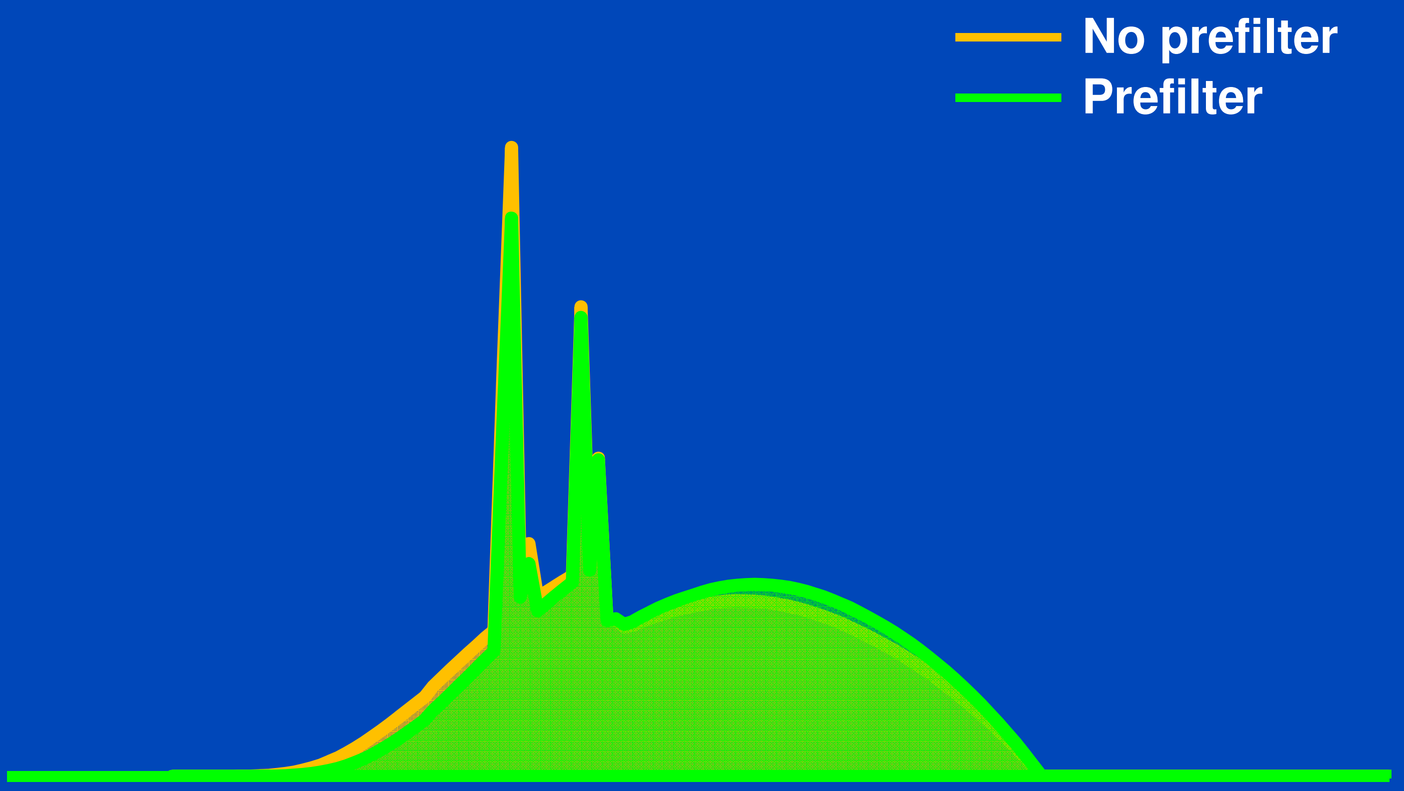

Beam Hardening

- **Measurement**

$$q = -\ln \int dE\, w(E) e^{-\int dL\, \mu(\boldsymbol{r}, E)}$$

- **Single material approximation:** $\mu(\boldsymbol{r}, E) = f_1(\boldsymbol{r})\psi_1(E)$

$$q = -\ln \int dE\, w(E) e^{-p_1 \psi_1(E)}$$

→ cupping, first order BH artifacts → cupping correction (water precorrection)

- **Two material case:** $\mu(\boldsymbol{r}, E) = f_1(\boldsymbol{r})\psi_1(E) + f_2(\boldsymbol{r})\psi_2(E)$

$$q = -\ln \int dE\, w(E) e^{-p_1 \psi_1(E) - p_2 \psi_2(E)}$$

→ banding artifacts, higher order BH artifacts → higher order BH correction

First Order Beam Hardening

32 cm Water Phantom

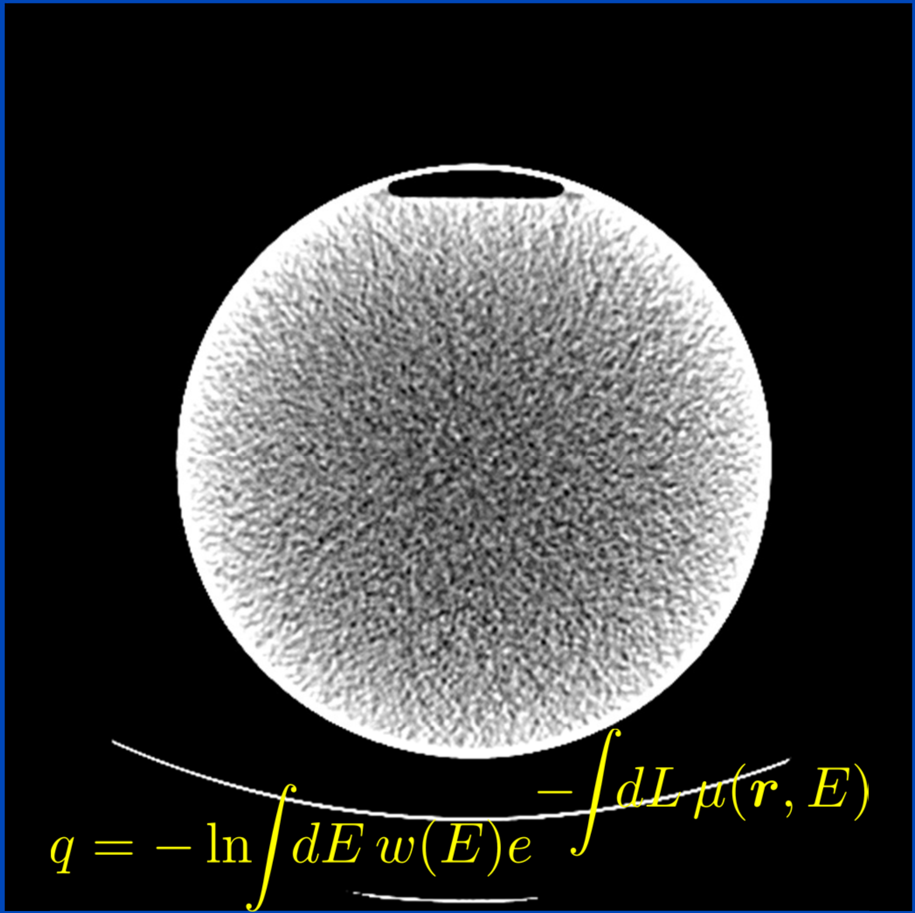

$$q = -\ln \int dE\, w(E) e^{-\int dL\, \mu(\boldsymbol{r}, E)}$$

Phantom with Water Precorrection

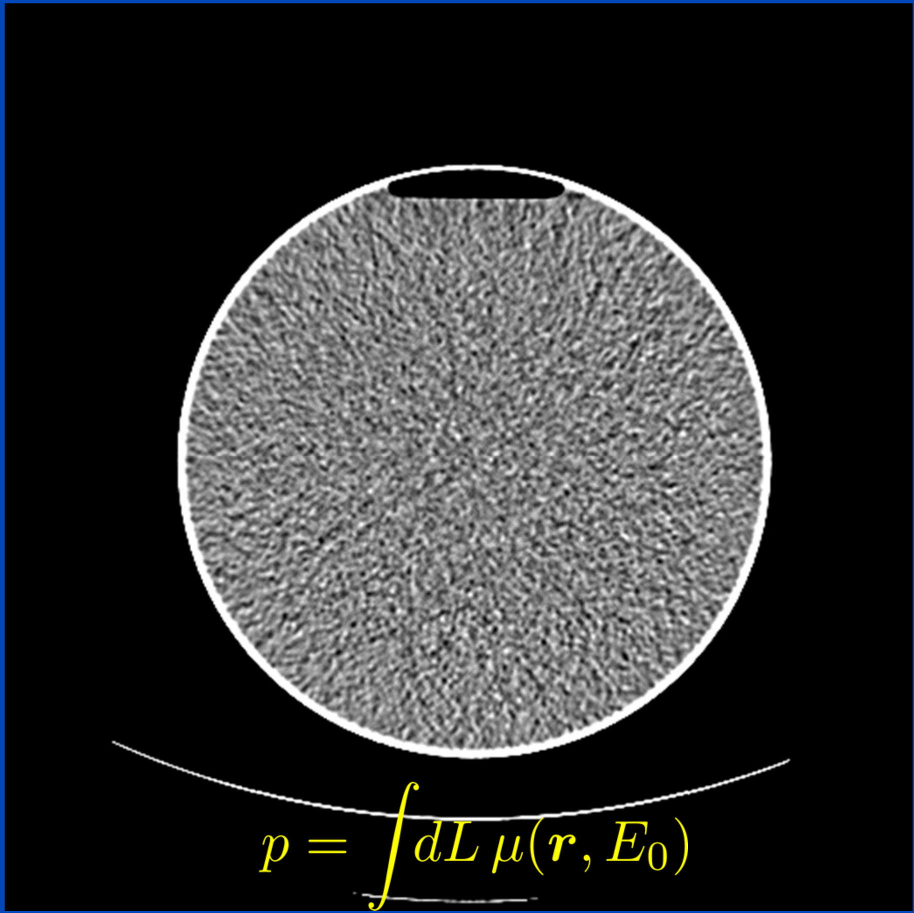

$$p = \int dL\, \mu(\boldsymbol{r}, E_0)$$

Water Precorrection: Determine a function *P* such that *p* = *P*(*q*) corrects for the cupping.

C = 0 HU, *W* = 100 HU

Analytical Cupping Correction

- **Know the detected spectrum, e.g.**

$$w(E) \propto E\, I(E)\,(1 - e^{-\mu_\mathrm{D}(E) d_\mathrm{D}})$$

- **Assume the object to be decomposed as**

$$\boxed{\mu(\boldsymbol{r}, E) = f(\boldsymbol{r})\psi(E)}$$

such that

$$q = -\ln \int dE\, w(E) e^{-\int dL\, p\, \psi(E)} \quad \textbf{with} \quad p = \int dL\, f(\boldsymbol{r})$$

- **Invert to get** $p = P(q)$

Empirical Cupping Correction (ECC)

- **Series expansion of the precorrection function**

$$p = P(q) = \sum_n c_n P_n(q) = \sum_n c_n q^n$$

- **Go to image domain by reconstructing *q^n***

$$f_n(\boldsymbol{r}) = \mathsf{X}^{-1} P_n(q) = \mathsf{X}^{-1} q^n$$

- **Find coefficients from**

$$f(\boldsymbol{r}) = \mathsf{X}^{-1} p = \mathsf{X}^{-1} P(q) = \sum_n c_n f_n(\boldsymbol{r})$$

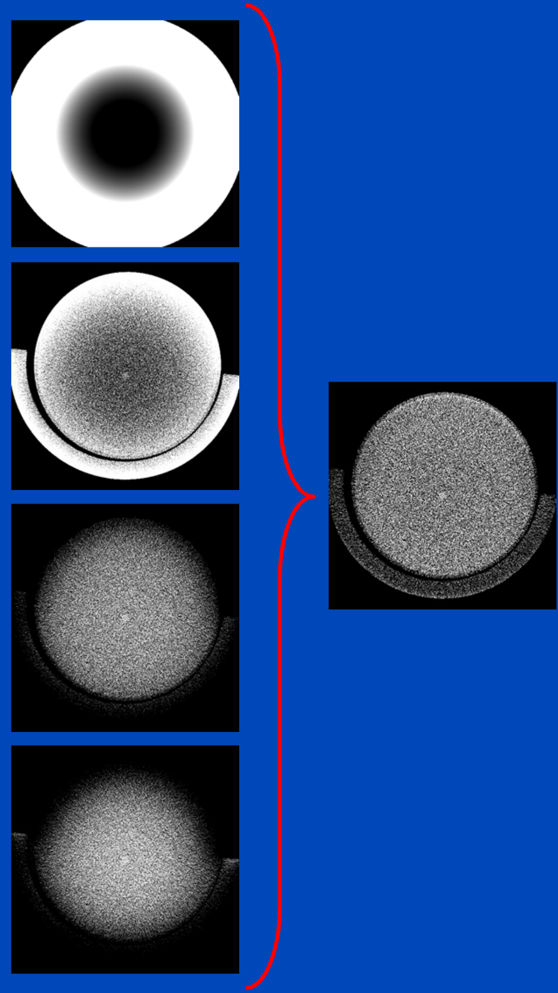

M. Kachelrieß, K. Sourbelle, and W.A. Kalender, "Empirical cupping correction: A first-order raw data precorrection for cone-beam computed tomography," Med. Phys. 33(5):1269-1274, May 2006.

ECC Template Image

$$\boldsymbol{c} = \arg\min_{\boldsymbol{c}} \int d^3r\, w(\boldsymbol{r})\big(f(\boldsymbol{r}) - t(\boldsymbol{r})\big)^2$$

$$f(\boldsymbol{r}) = \sum_n c_n f_n(\boldsymbol{r})$$

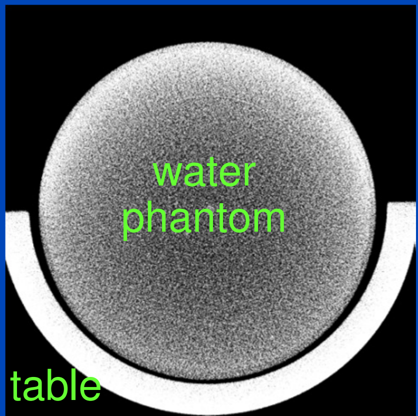

Original image
$f_1(\boldsymbol{r})$

segment and
specify CT-values

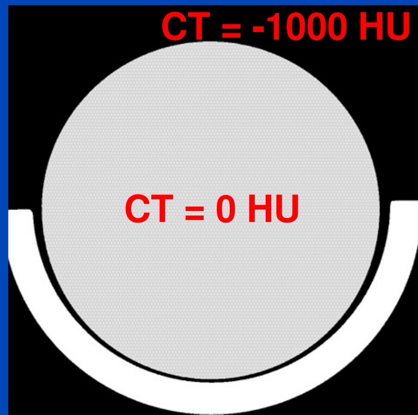

Template image
$t(\boldsymbol{r})$

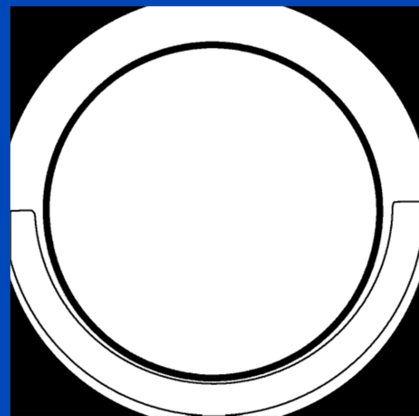

Weight image
$w(\boldsymbol{r})$

M. Kachelrieß, K. Sourbelle, and W.A. Kalender, "Empirical cupping correction: A first-order raw data precorrection for cone-beam computed tomography," Med. Phys. 33(5):1269-1274, May 2006.

Results: Water Phantom

Orig (Mean±4Sigma)

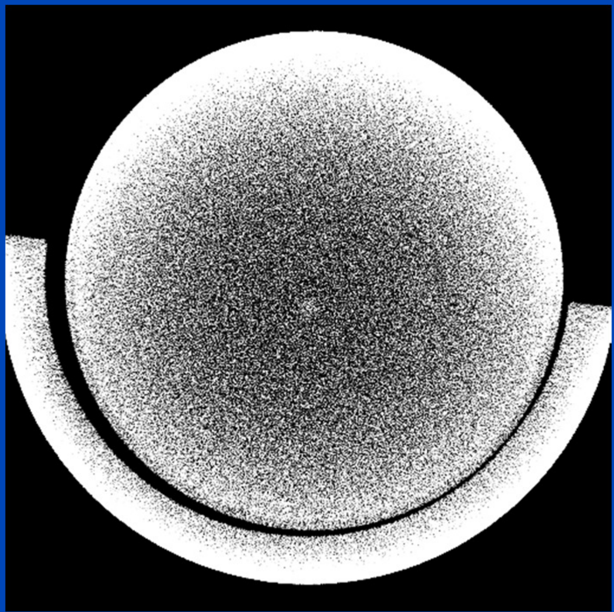

ECC (Mean±4Sigma)

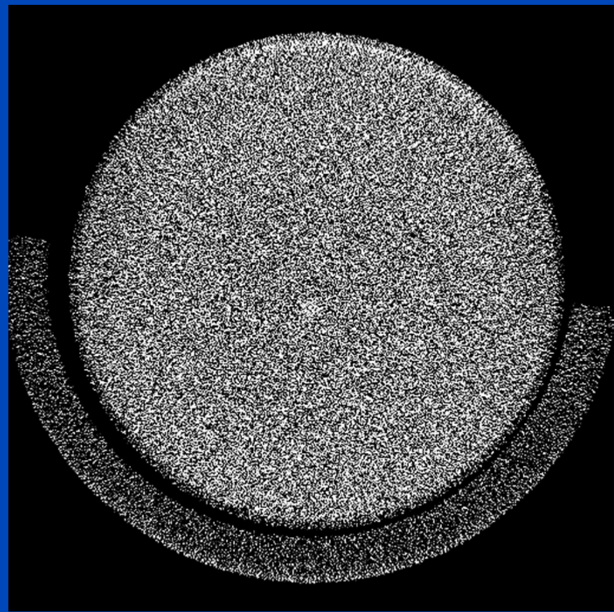

M. Kachelrieß, K. Sourbelle, and W.A. Kalender, "Empirical cupping correction: A first-order raw data precorrection for cone-beam computed tomography," Med. Phys. 33(5):1269-1274, May 2006.

Results: Mouse Scan

No correction (Mean±4Sigma)

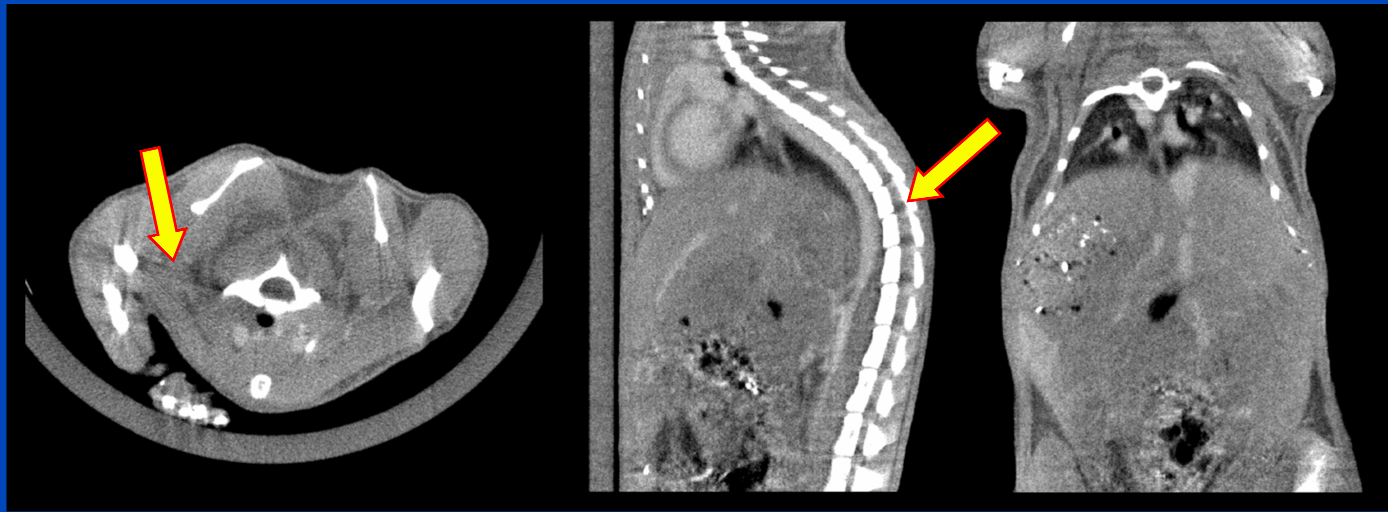

ECC (Mean±4Sigma)

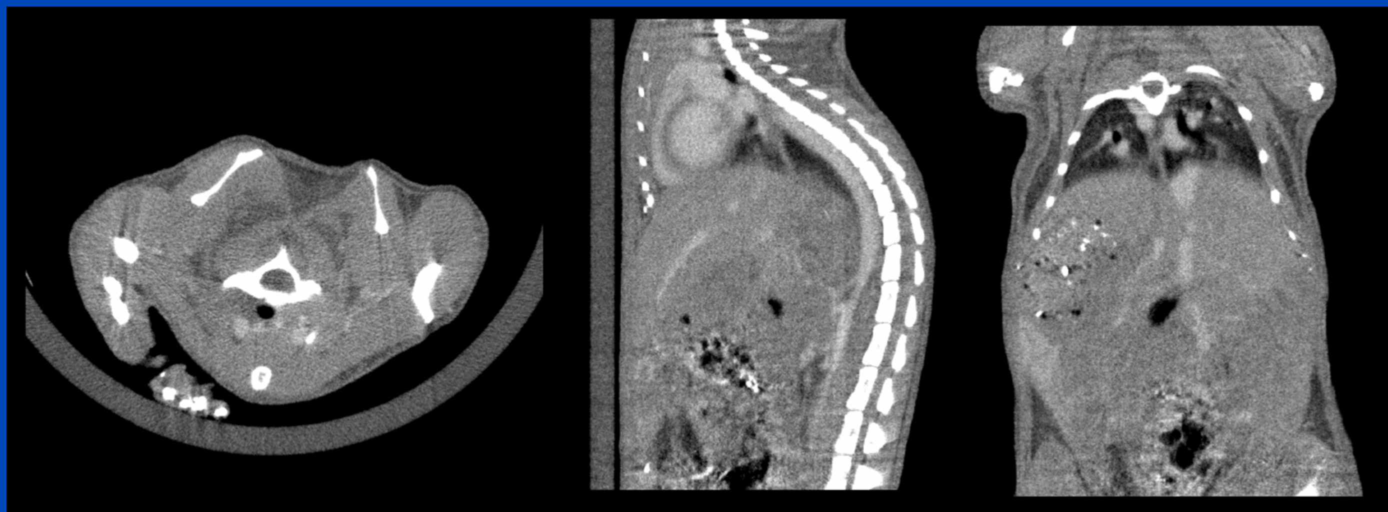

M. Kachelrieß, K. Sourbelle, and W.A. Kalender, “Empirical cupping correction: A first-order raw data precorrection for cone-beam computed tomography,” Med. Phys. 33(5):1269-1274, May 2006.

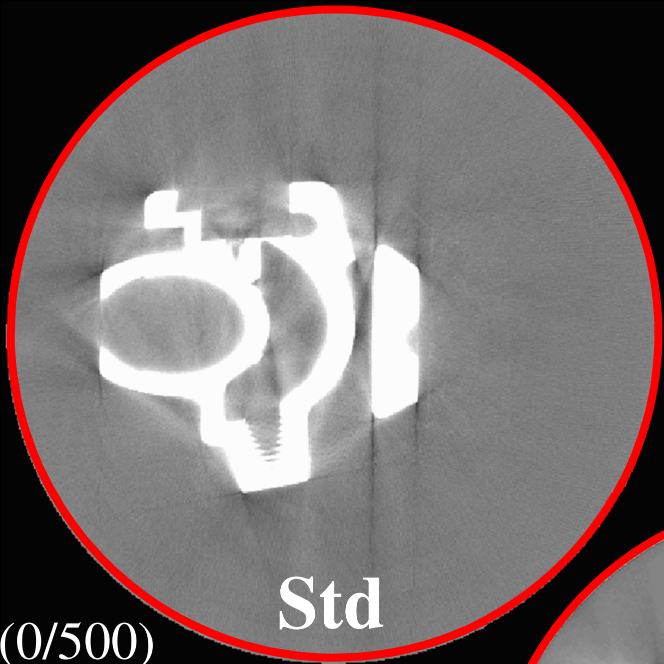

(0/500)

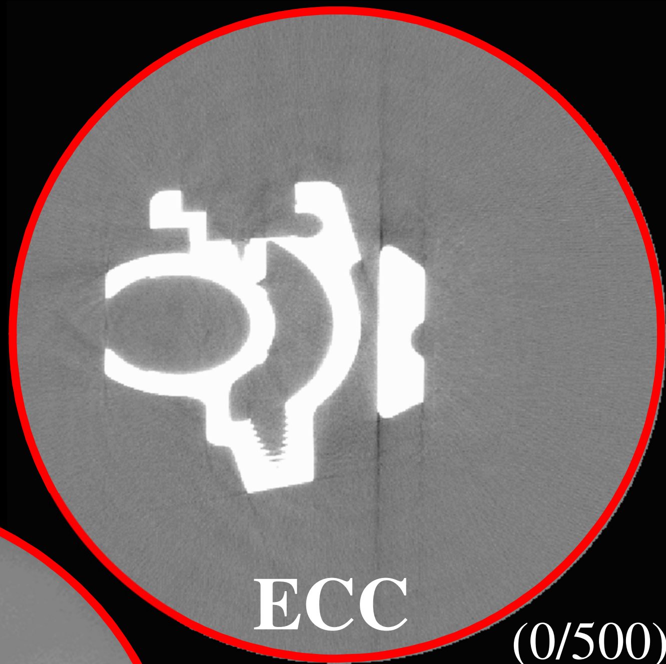

(0/500)

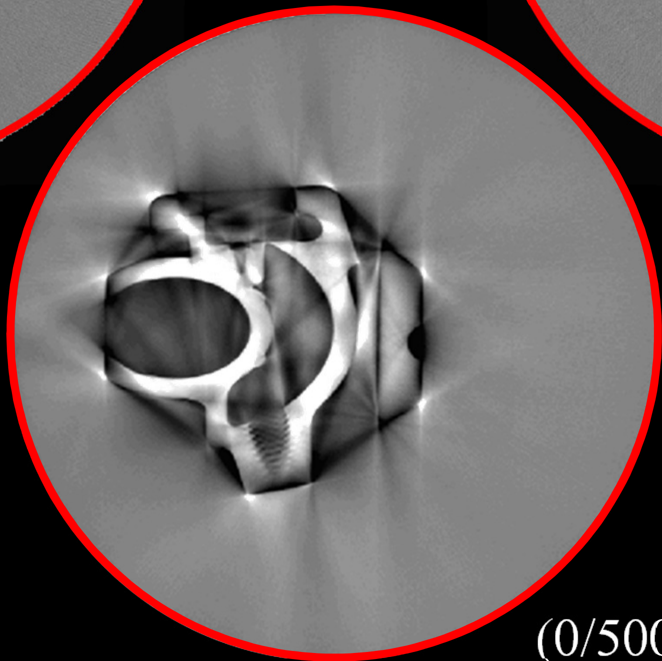

(0/500)

CT Metrology

M. Kachelrieß, K. Sourbelle, and W.A. Kalender, "Empirical cupping correction: A first-order raw data precorrection for cone-beam computed tomography," Med. Phys. 33(5):1269-1274, May 2006.

Std

(1000/200)

ECC

(1000/200)

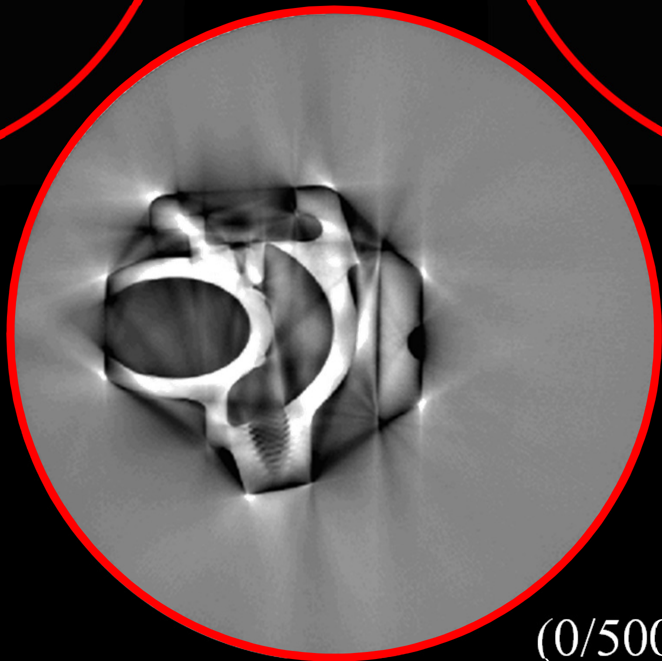

(0/500)

CT Metrology

M. Kachelrieß, K. Sourbelle, and W.A. Kalender, “Empirical cupping correction: A first-order raw data precorrection for cone-beam computed tomography,” Med. Phys. 33(5):1269-1274, May 2006.

Higher Order Beam Hardening

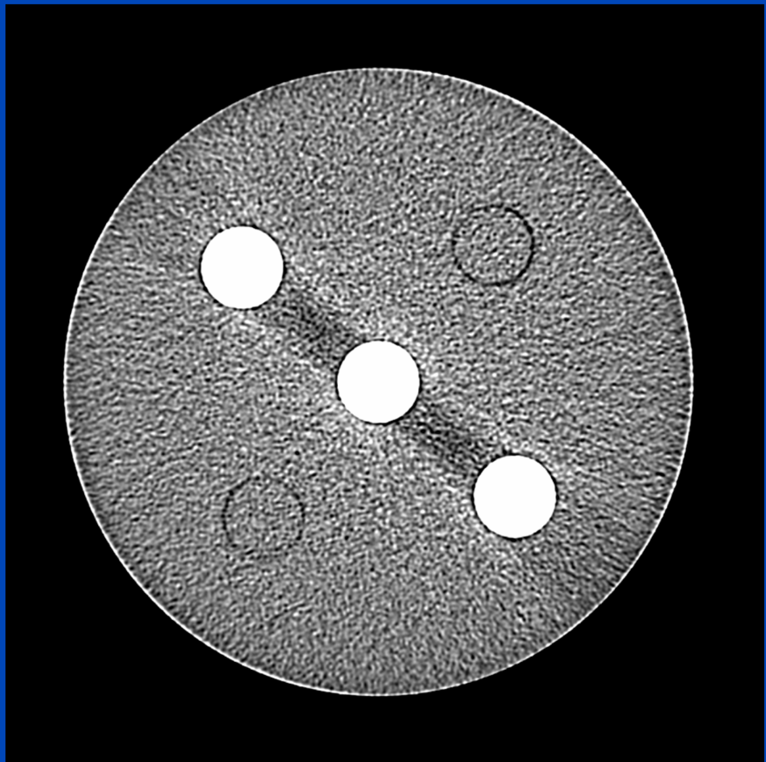

Image domain algorithms, such as the scaling method, do not account for higher order beam hardening effects. They can recover the attenuation correction factors (ACF) only to a first order of approximation.

M. Kachelrieß, and W.A. Kalender, “Improving PET/CT attenuation correction with iterative CT beam hardening correction,” IEEE Medical Imaging Conference Program, M04-5, October 2005.

Energy Dependence of Attenuation

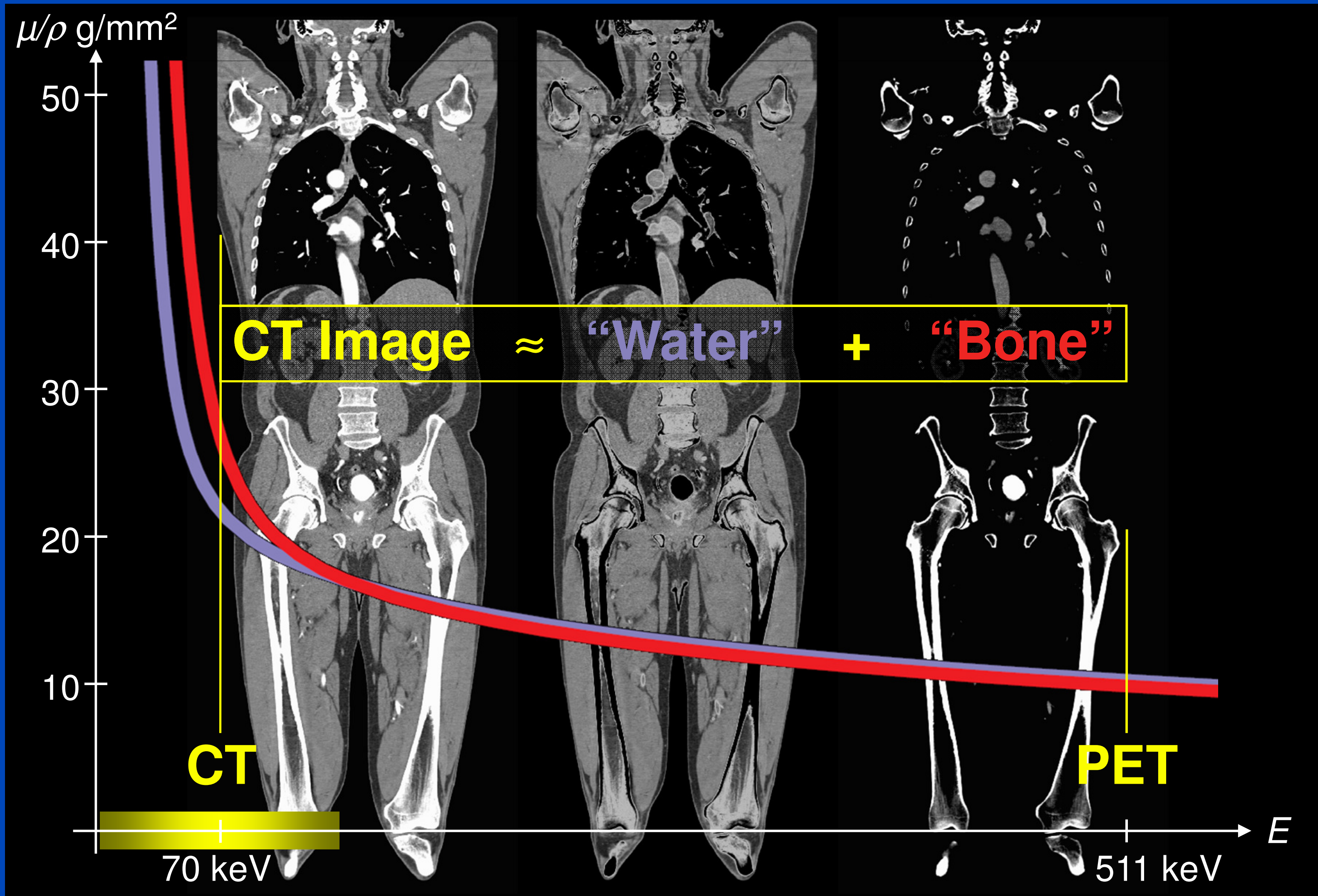

M. Kachelrieß, and W.A. Kalender, "Improving PET/CT attenuation correction with iterative CT beam hardening correction," IEEE Medical Imaging Conference Program, M04-5, October 2005.

dkfz.

Many Materials
(typically requires iterative BHC)

- **Assume** $$\mu(E,\boldsymbol{r}) = \sum_i \psi_i(E) g_i(\boldsymbol{r}) = \boldsymbol{\psi}(E)\cdot\boldsymbol{g}(\boldsymbol{r})$$
- **Let** $$q = \mathsf{X}_g g = -\ln \int dE\, w(E) e^{-\boldsymbol{\psi}(E)\cdot\boldsymbol{p}}$$

  with $$p_i = \mathsf{X} g_i = \int dL\, g_i(\boldsymbol{r})$$
- **For beam hardening correction we need to recover *$g_i(r)$* for all materials present. Then we can convert to any desired *E_0* as**

$$\mu(E_0,\boldsymbol{r}) = \sum_i \psi_i(E_0) g_i(\boldsymbol{r})$$

M. Kachelrieß, and W.A. Kalender, "Improving PET/CT attenuation correction with iterative CT beam hardening correction," IEEE Medical Imaging Conference Program, M04-5, October 2005.

Iterative BHC

initial water-precorrected CT image (or rawdata)

desired BHC-corrected CT image

$$\mathsf{X}_f f = \mathsf{X}_g g$$

$$\mathsf{B}_f f = \mathsf{B}_g g = g - (1 - \mathsf{B}_g) g$$

$$g = \mathsf{B}_f f + (1 - \mathsf{B}_g) g$$

with

$$\mathsf{B}_f = \mathsf{X}^{-1}\mathsf{X}_f$$

$$\mathsf{B}_g = \mathsf{X}^{-1}\mathsf{X}_g$$

Numerically superior expressions:

$$g = f + (\mathsf{B}_f - \mathsf{B}) f + (\mathsf{B} - \mathsf{B}_g) g \quad \text{with} \quad \mathsf{B} = \mathsf{X}^{-1}\mathsf{X}$$

$$\boxed{g^{(n+1)} = f + (\mathsf{B}_f - \mathsf{B}) f + (\mathsf{B} - \mathsf{B}_g) g^{(n)} \quad \text{with} \quad g^{(0)} = f}$$

Shortcut: $g^{(1)} = f + \mathsf{X}^{-1}(\mathsf{X}_f - \mathsf{X}_g) f$

M. Kachelrieß, and W.A. Kalender, “Improving PET/CT attenuation correction with iterative CT beam hardening correction,” IEEE Medical Imaging Conference Program, M04-5, October 2005.

dkfz.

Phantom Measurements
Spiral 64-Slice CT Scan at 120 kV

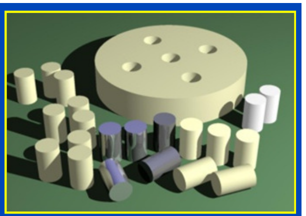

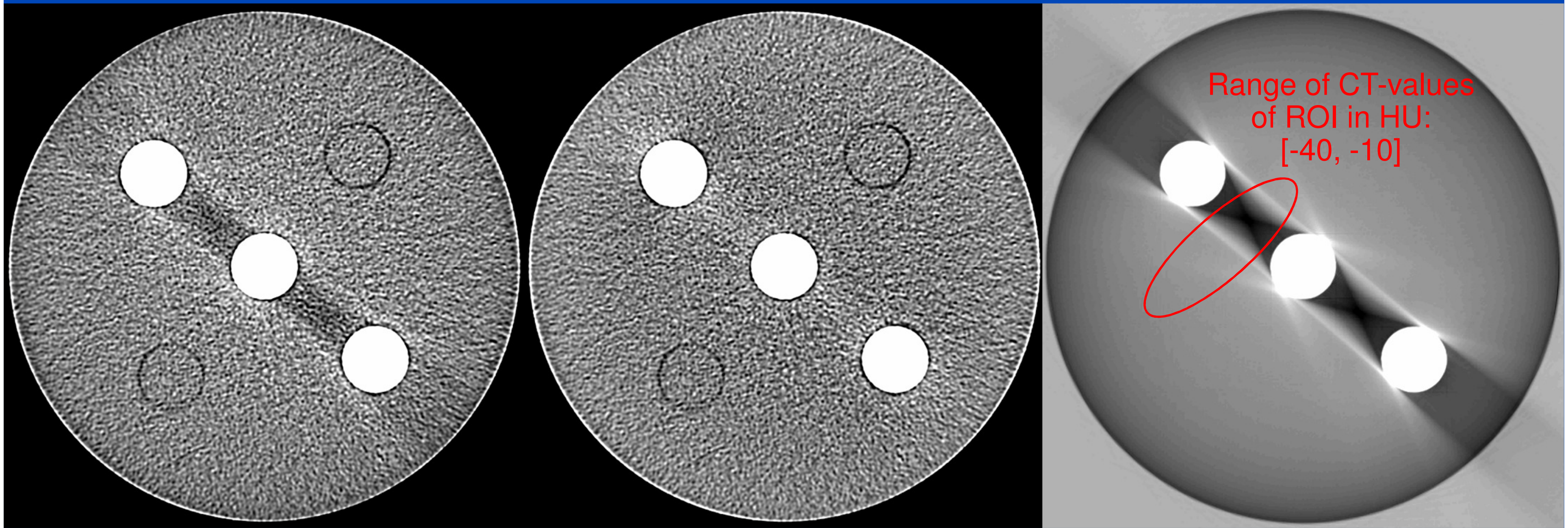

Original Image	BHC Image	Original minus BHC
(C = -80, W = 100)	(C = -70, W = 100)	(C = -10, W = 50)

- 20 cm PE disk phantom with three 3 cm HA400 inserts
- BH artifacts apparent even for this small phantom
- BHC removes capping
- BHC removes dark streaks
- BHC recovers the true CT values

$$\rho_{PE} = 0.93\,\rho_W = -70\text{ HU}$$
$$\rho_{HA400} = 1.27\,\rho_W = 270\text{ HU}$$

M. Kachelrieß, and W.A. Kalender, "Improving PET/CT attenuation correction with iterative CT beam hardening correction," IEEE Medical Imaging Conference Program, M04-5, October 2005.

Patient Data

Spiral 4-Slice CT Scan at 120 kV

Original Image | **BHC Image** | **Original minus BHC**

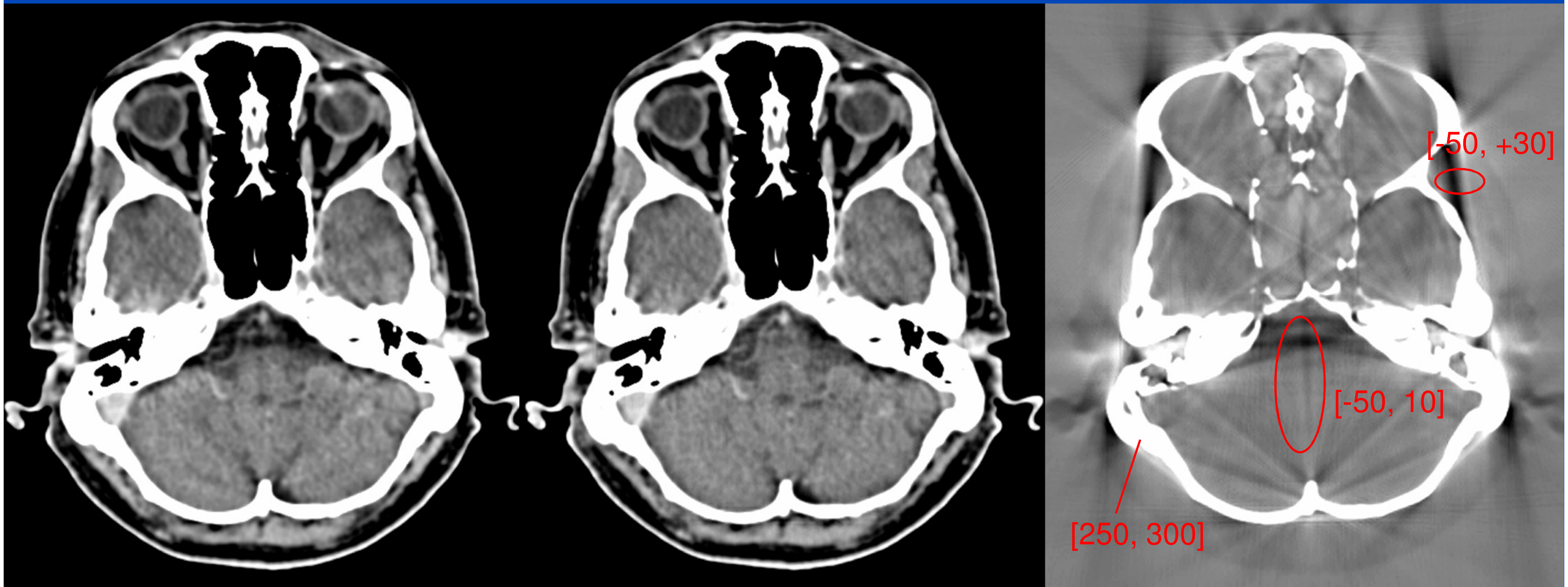

(C = 40, W = 150)

(C = 0, W = 100)

Red values indicate the range of CT-values within the corresponding ROI in HU

M. Kachelrieß, and W.A. Kalender, "Improving PET/CT attenuation correction with iterative CT beam hardening correction," IEEE Medical Imaging Conference Program, M04-5, October 2005.

Empirical Beam Hardening Correction (EBHC)

- **Requirements/Objectives**
  - Empirical correction of <u>higher order</u> beam hardening effects
  - No assumptions on attenuation coefficients, spectra, detector responses or other properties of the scanner
  - Image-based and system-independent method

- **Overview of correction steps**
  - Forward project segmented bone volume to obtain artificial rawdata
  - Pass the artificial rawdata through basis functions
  - Reconstruct the basis functions
  - Linearly combine the correction volumes and the original volume using flatness maximization

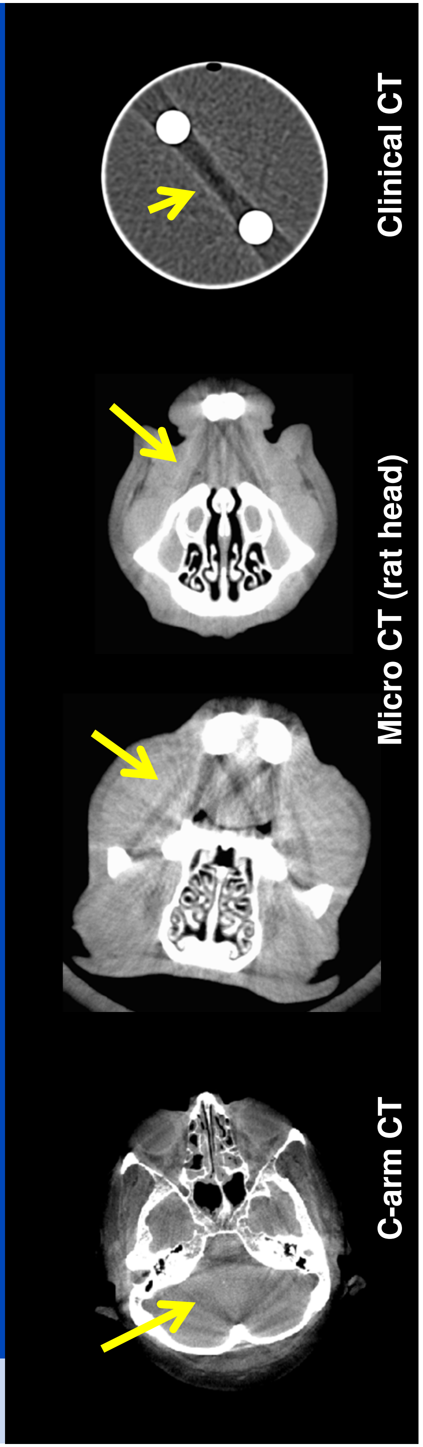

Y. Kyriakou, E. Meyer, D. Prell, and M. Kachelrieß, "Empirical beam hardening correction (EBHC) for CT," Med. Phys. 37(10):5179-5187, October 2010.

EBHC Details

- **Decomposition into an effective water-equivalent density $\hat{f}_1(r)$ of the object and into an effective energy dependence $\hat{\psi}_2(E)$ of a second material, e.g. bone**

$$\begin{aligned}\mu(\boldsymbol{r},E) &= f_1(\boldsymbol{r})\psi_1(E) + f_2(\boldsymbol{r})\psi_2(E)\\ &= \big(f_1(\boldsymbol{r}) + f_2(\boldsymbol{r})\big)\psi_1(E) + f_2(\boldsymbol{r})\big(\psi_2(E) - \psi_1(E)\big)\\ &= \hat{f}_1(\boldsymbol{r})\psi_1(E) + f_2(\boldsymbol{r})\hat{\psi}_2(E).\end{aligned}$$

- **Assuming water-precorrected data gives**

$$\int dE\, w(E) e^{-p_0\psi_0(E)} = \int dE\, w(E) e^{-\hat{p}_1\psi_1(E) - p_2\hat{\psi}_2(E)}$$

where $\hat{p}_1$ and p_2 are the line integrals through $\hat{f}_1(r)$ and $f_2(r)$

Y. Kyriakou, E. Meyer, D. Prell, and M. Kachelrieß, "Empirical beam hardening correction (EBHC) for CT," Med. Phys. 37(10):5179-5187, October 2010.

EBHC Details

- We solve for $\hat{p}_1(r)$ using a series expansion

$$\hat{p}_1(p_0, p_2) = \sum_{ij} c_{ij} p_0^i p_2^j = p_0 + c_{01} p_2 + c_{11} p_0 p_2 + c_{02} p_2^2 + \ldots$$

$\mathbf{R}^{-1}$ $\mathbf{R}^{-1}$ $\mathbf{R}^{-1}$

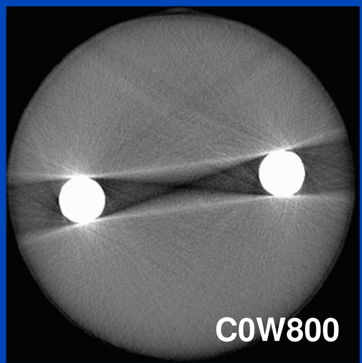

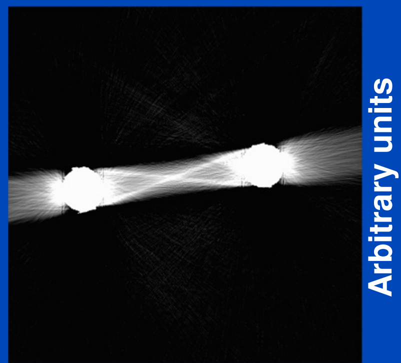

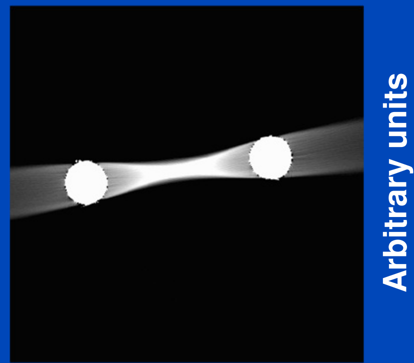

- Empirically find c_{11} and c_{02} to correct initial image by flatness maximization

Y. Kyriakou, E. Meyer, D. Prell, and M. Kachelrieß, "Empirical beam hardening correction (EBHC) for CT," Med. Phys. 37(10):5179-5187, October 2010.

EBHC for Clinical CT

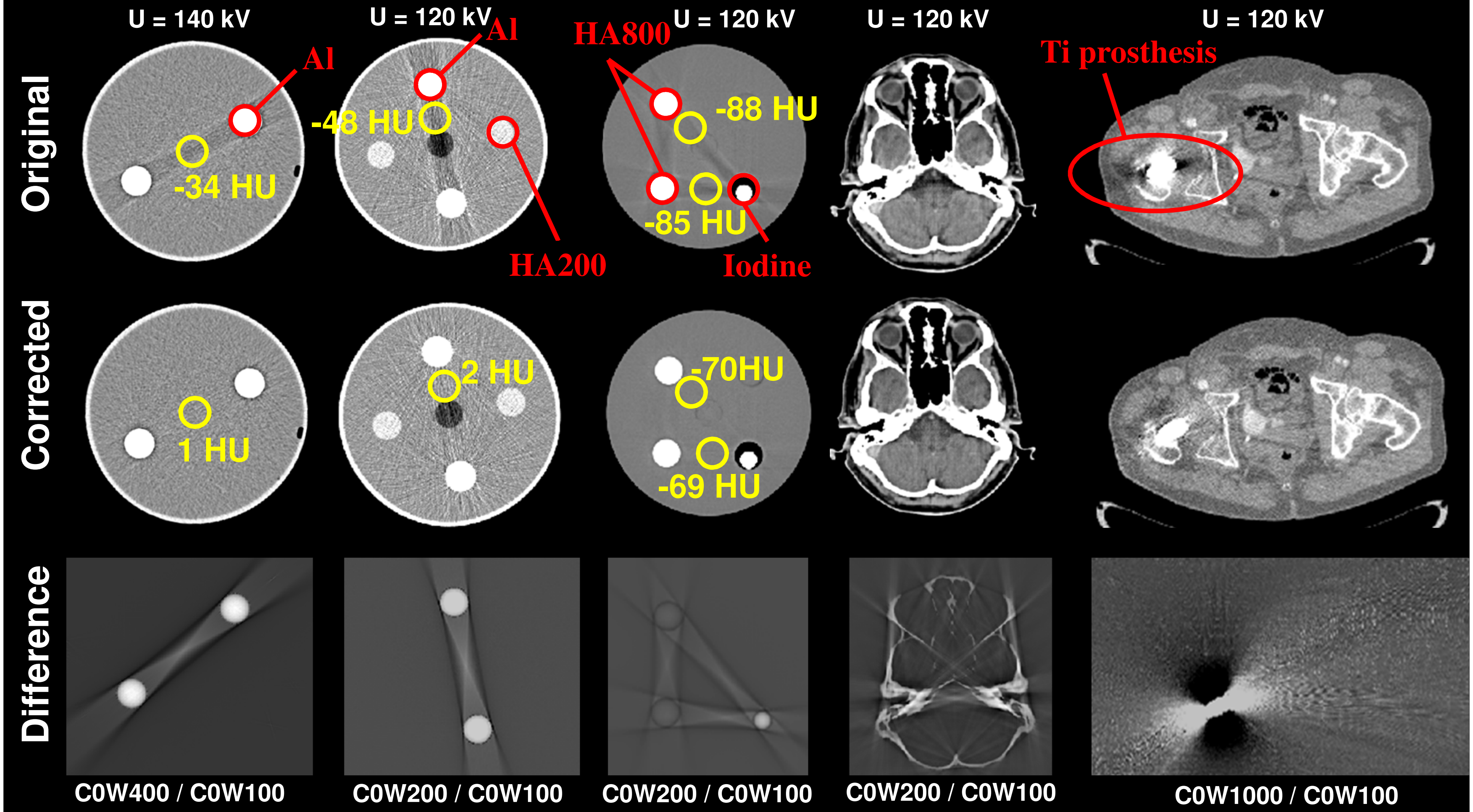

Y. Kyriakou, E. Meyer, D. Prell, and M. Kachelrieß, "Empirical beam hardening correction (EBHC) for CT," Med. Phys. 37(10):5179-5187, October 2010.

EBHC for Micro CT

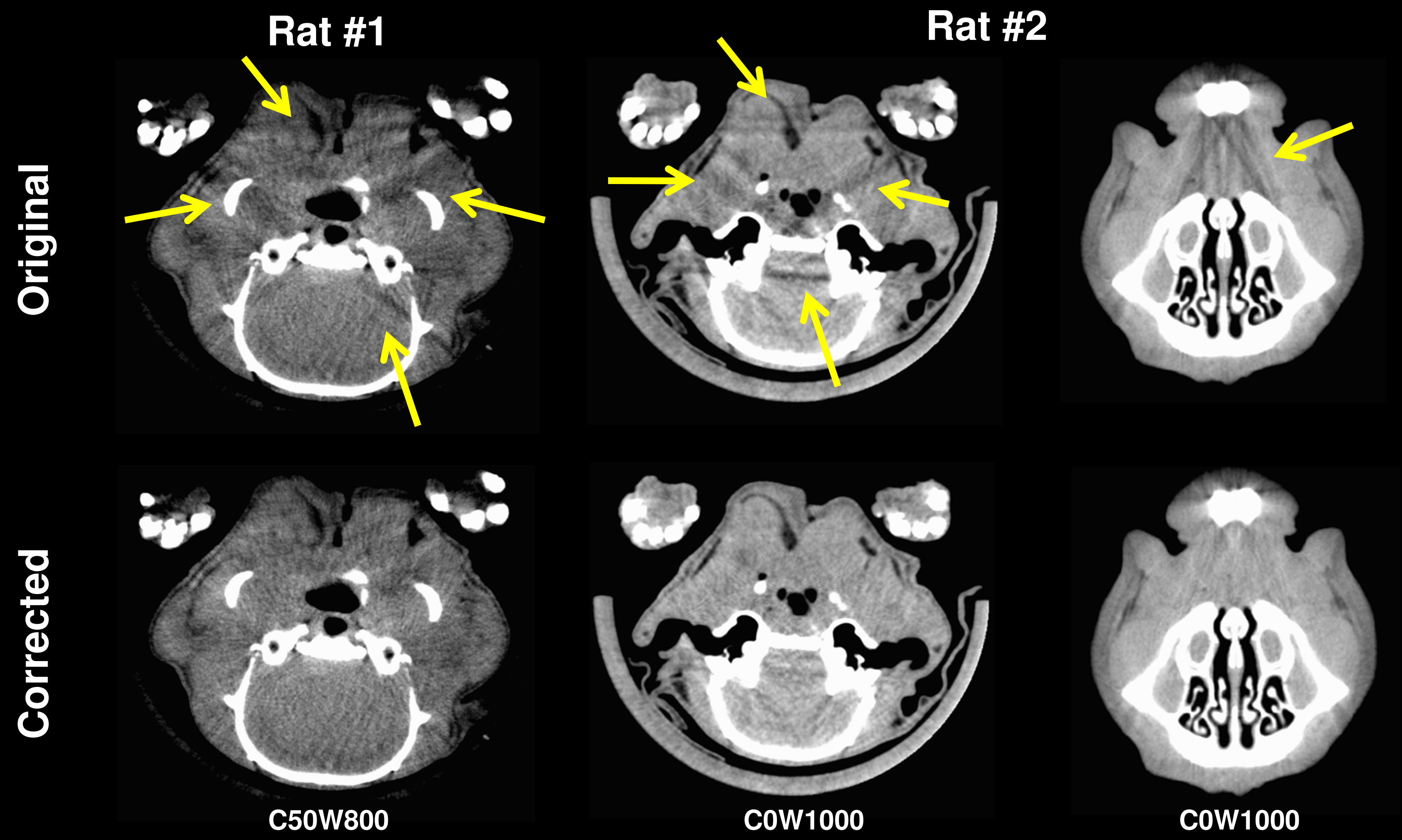

Y. Kyriakou, E. Meyer, D. Prell, and M. Kachelrieß, “Empirical beam hardening correction (EBHC) for CT,” Med. Phys. 37(10):5179-5187, October 2010.

EBHC: Clinical CT vs. FD-CT

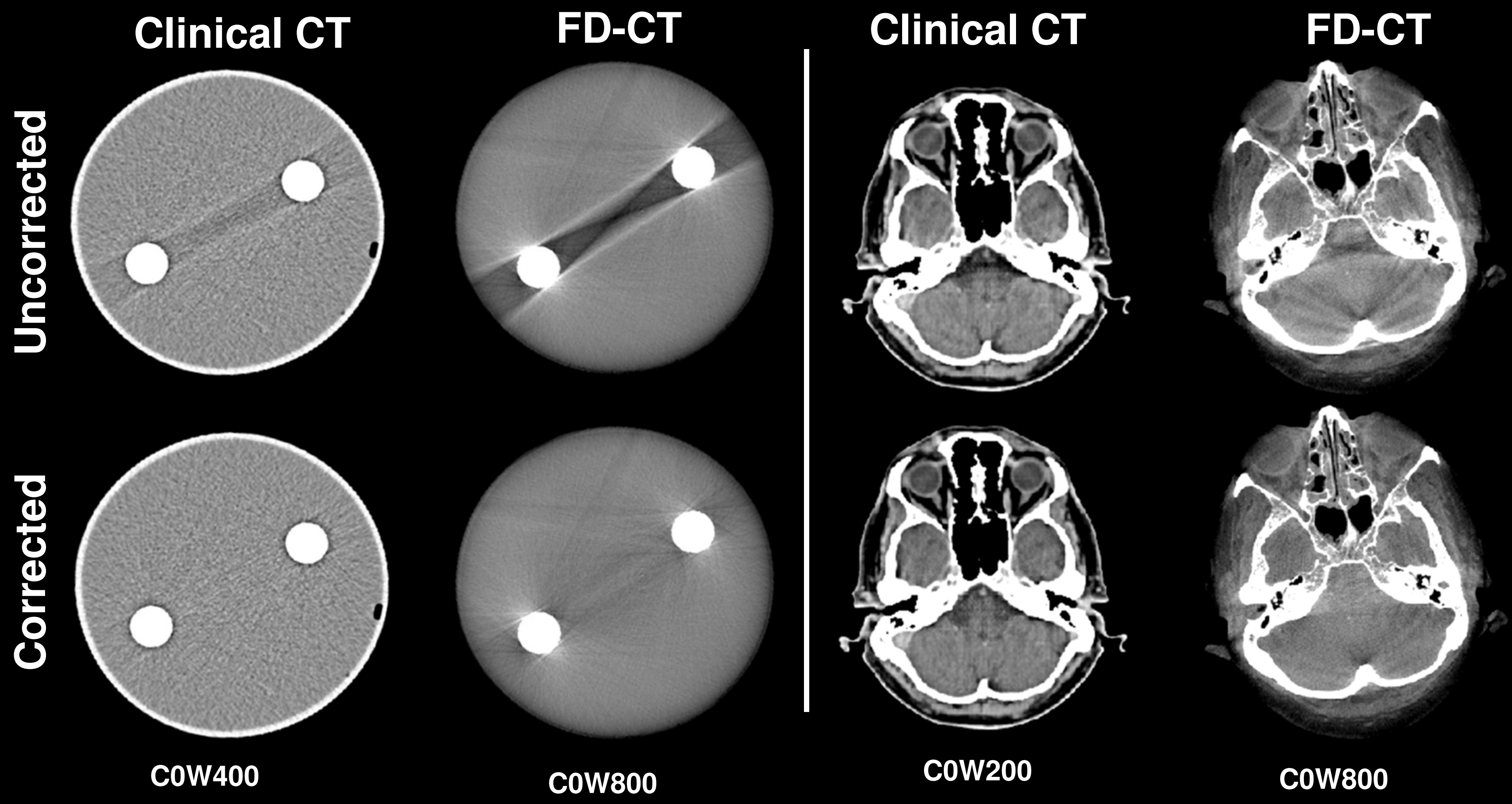

Y. Kyriakou, E. Meyer, D. Prell, and M. Kachelrieß, “Empirical beam hardening correction (EBHC) for CT,” Med. Phys. 37(10):5179-5187, October 2010.

Further Reading

- Yunsong Zhao, and Mengfei Li. Iterative Beam Hardening Correction for Multi-Material Objects. PLoS ONE 10(12):1-13, December 2015.
- Hyoung Suk Park, Dosik Hwang, and Jin Keun Seo. Metal Artifact Reduction for Polychromatic X-ray CT Based on a Beam-Hardening Corrector. IEEE TMI 35(2):480-487, September 2015.
- Rune Slot Thing, Uffe Bernchou, Ernesto Mainegra-Hing, Olfred Hansen, and Carsten Brink. Hounsfield unit recovery in clinical cone beam CT images of the thorax acquired for image guided radiation therapy. Phys. Med. Biol. 61(15):5781-5802, July 2016.

Scatter Artifact Reduction

- Several algorithmic methods found in the literature:
  - Monte Carlo-based (slow but good)
  - Convolution-based (fast, but not accurate)
  - Simple subtraction methods (even faster, but less accurate)
  - …
- Hardware-based methods
  - Anti scatter grid
  - Beam blockers
  - Primary modulators
  - …

Scatter Estimation

Monte Carlo-based

Measured intensities (primary plus scatter)

Reconstruction

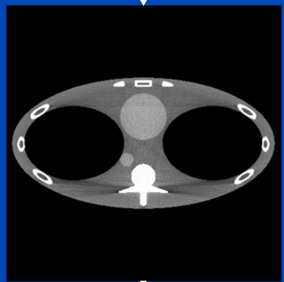

Simulation of physical photon paths based on density and material distribution

Physical effects:
Photo effect
Compton scattering
Rayleigh scattering

Monte Carlo-based scatter estimate $\hat{I}_{\mathrm{s}}^{\mathrm{MC}}$

Patient-specific, many computations

Convolution-based

Measured intensities (primary plus scatter)

$$\hat{I}_{\mathrm{s}}^{\mathrm{CB}}(\boldsymbol{c}) = \Phi\big(I_{\mathrm{ps}}, \boldsymbol{c}\big) * K(\boldsymbol{c})$$

Convolution of the scatter potential Φ with scatter kernel K

I_{ps}: Primary plus scatter intensity

c (vector): Open coefficients

We used the convolution-based method of Ohnesorge et al.*

Convolution-based scatter estimate $\hat{I}_{\mathrm{s}}^{\mathrm{CB}}$

Not patient-specific, few computations

* Ohnesorge et al., Efficient scatter correction algorithm for third and fourth generation CT scanners, Eur. Radiol., 9, 563-569 (1999).

Hybrid Scatter Correction

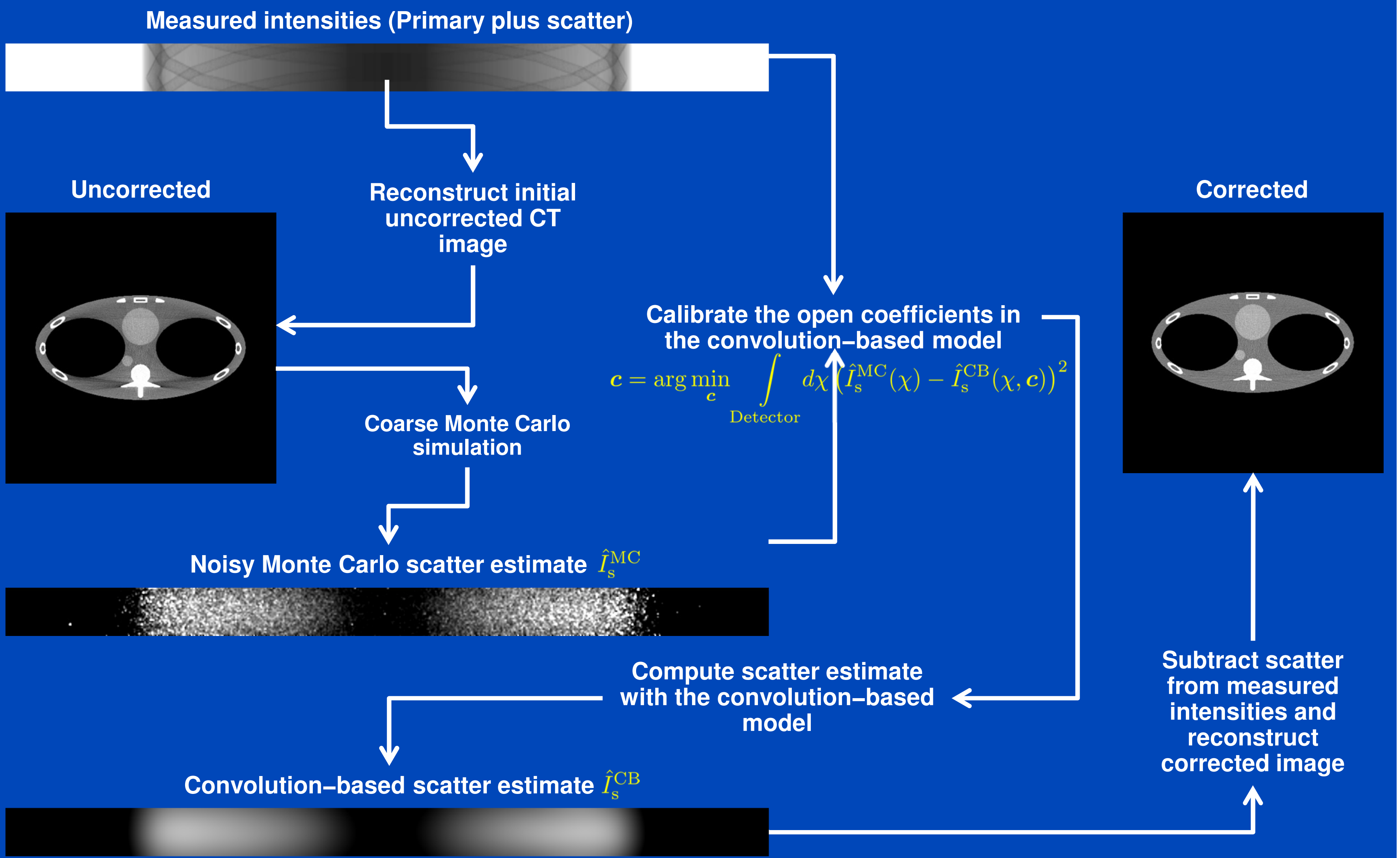

Number of Calibration Steps

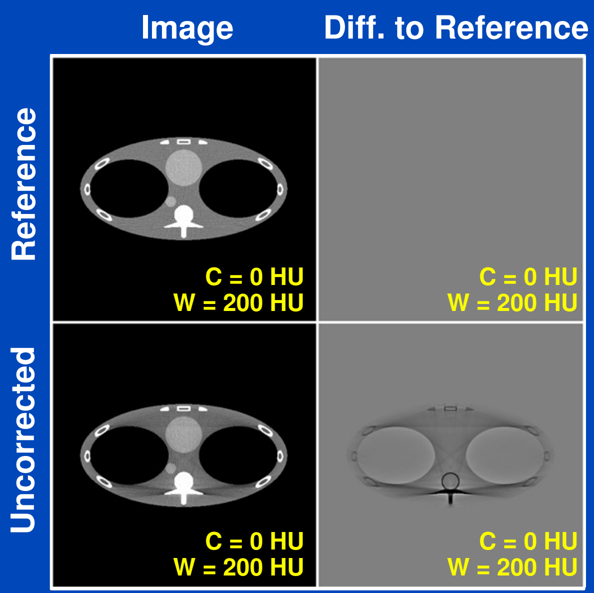

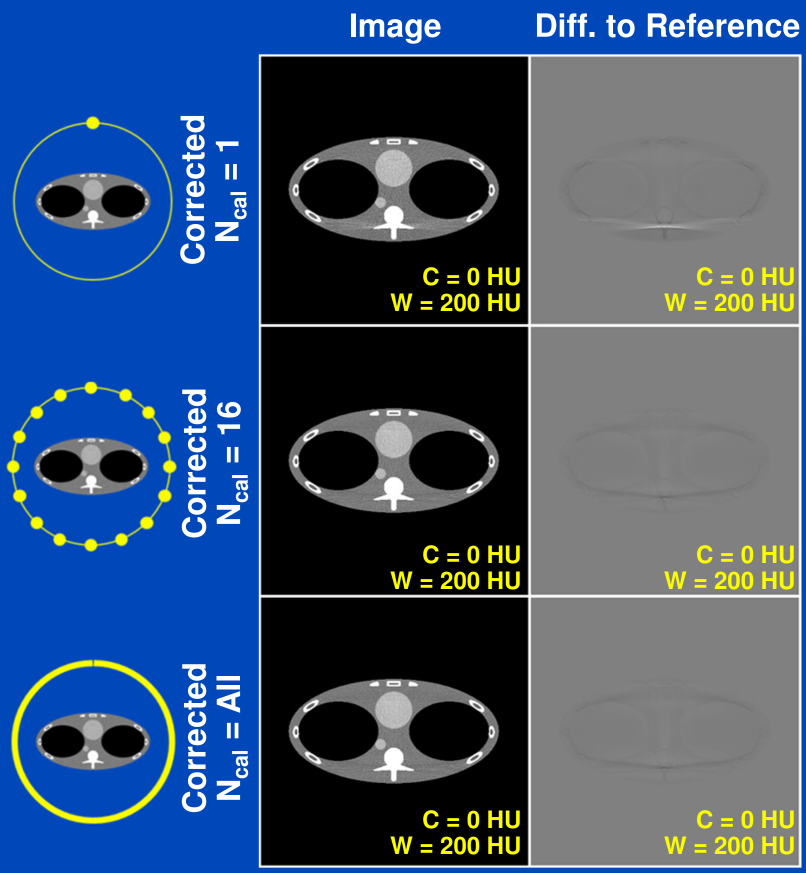

Monochromatic simulation study in clinical CT geometry
Scatter simulation by Monte Carlo

M. Baer and M. Kachelrieß. Hybrid scatter correction for CT imaging.
Phys. Med. Biol. 57(21):6849-6867, October 2012.

Number of Photons

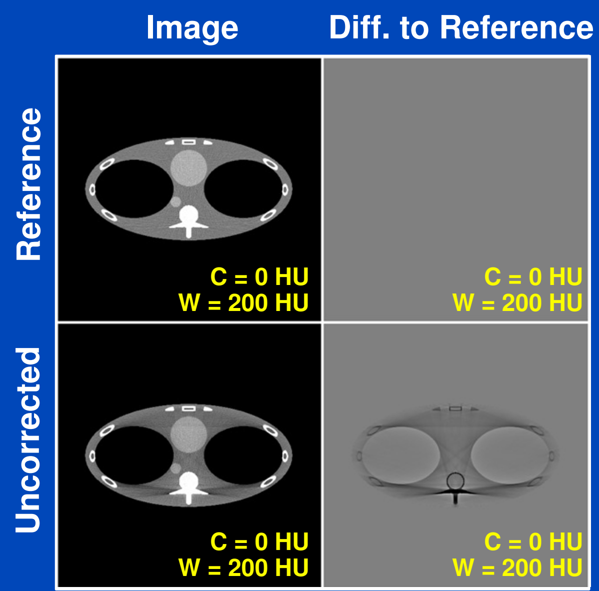

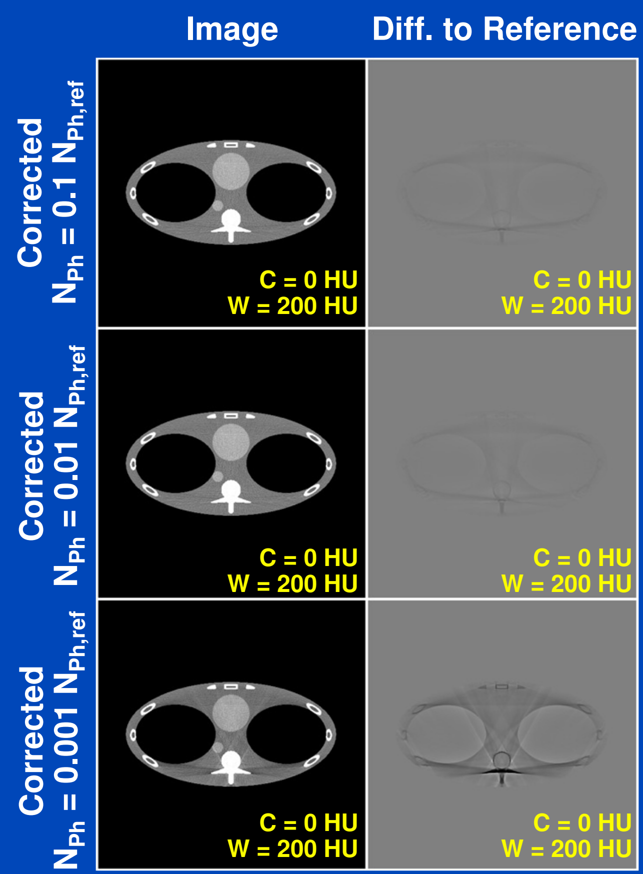

Monochromatic simulation study in clinical CT geometry
Scatter simulation by Monte Carlo

$N_{Ph,ref}$: Photon number for the low noise reference Monte Carlo simulation used for the uncorrected image

$N_{cal} = 16$

Scatter Correction Results

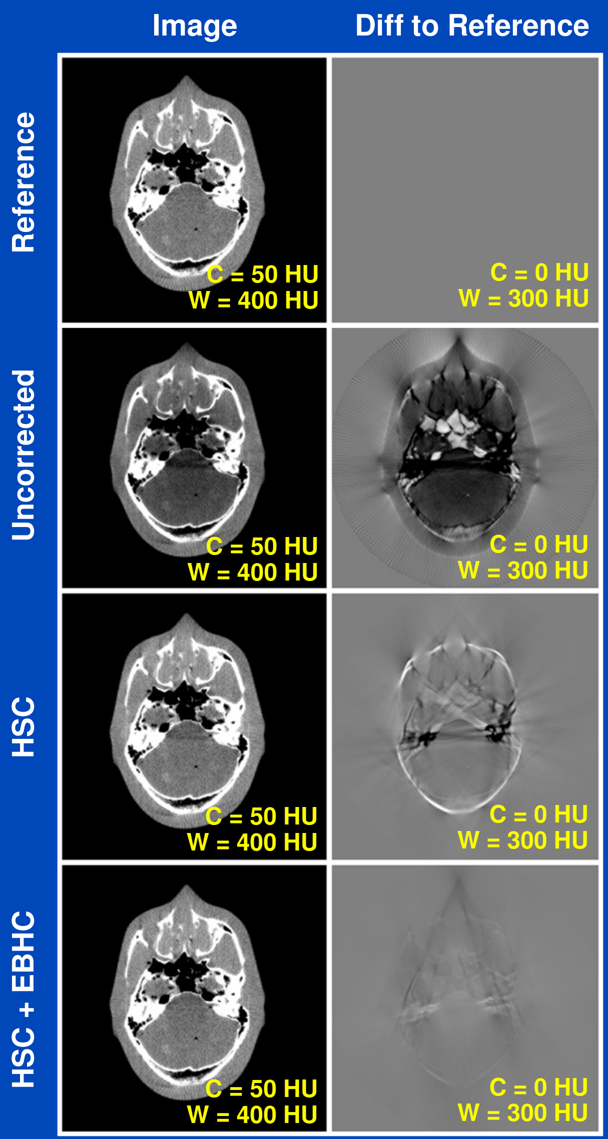

Measurements in cone-beam CT geometry

Reference image:
Pure Monte Carlo scatter correction and EBHC for beam hardening.

Hybrid scatter correction (HSC):
Monte Carlo simulation for only 16 projections and 100 times less photons than in the pure Monte Carlo correction.

Additionally the empirical beam-hardening correction (EBHC*) method was applied to correct for beam-hardening artifacts.

*Kyriakou, Y.; Meyer, E.; Prell, D.; Kachelrieß, M.;
Empirical Beam Hardening Correction (EBHC) for CT, Med. Phys. 37, 5179-87 (2010).

Further Reading

- Wei Zhao, Don Vernekohl, Jun Zhu, Luyao Wang, and Lei Xing. A model-based scatter artifacts correction for cone beam CT. Medical Physics 43 (1736), March2016.
- Ernst-Peter Rührnschopf and Klaus Klingenbeck. A General Framework and Review of Scatter Correction Methods in X-Ray Cone-Beam Computerized Tomography. Part 1: Scatter Compensation Approaches. Med. Phys. 38(7):4296-4311, July 2011.
- Ernst-Peter Rührnschopf and Klaus Klingenbeck. A General Framework and Review of Scatter Correction Methods in X-Ray Cone-Beam Computerized Tomography. Part 2: Scatter Estimation Approaches. Med. Phys. 38(9):5186-5199, September 2011.

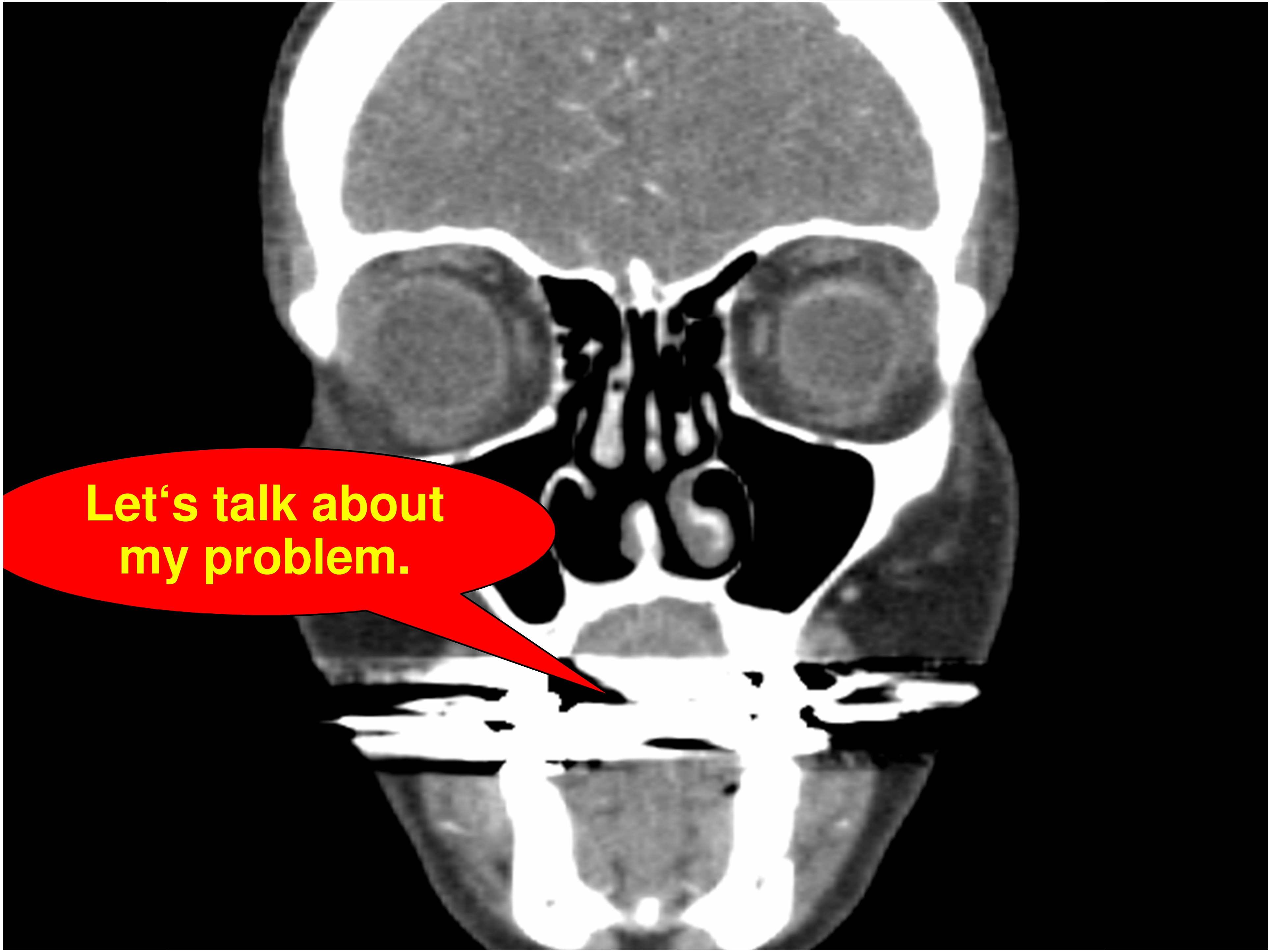
Let‘s talk about
my problem.

Metal Artifacts are

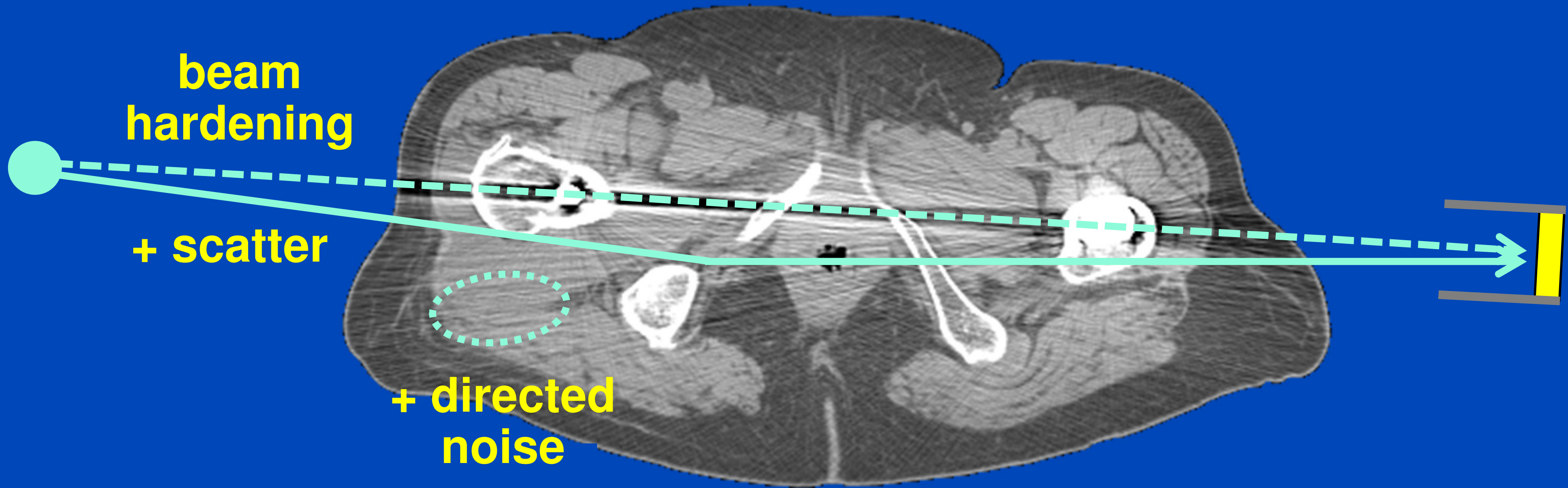

+ increased susceptibility to sampling artifacts and motion.

Metal Artifact Reduction (MAR)

- Physics-based metal artifact reduction (not discussed here – my colleague Joscha Maier gave sufficient details on Wednesday) should comprise beam hardening correction, scatter correction, and corrections for the beam shape and sampling.
- MAR typically refers to inpainting the projection values that are influenced by the metal. This is a hollow projection problem and completely ignores the underlying physics.
- Detect metal contents
  - in image domain (very reliable, simple thresholding suffices)
  - in rawdata domain (not reliable, but many attempts)
- Inpaint the hollow projections
  - by simple interpolation
  - by sophisticated anisotropic methods
  - with or without normalization techniques.

Linear Interpolation MAR (LIMAR)

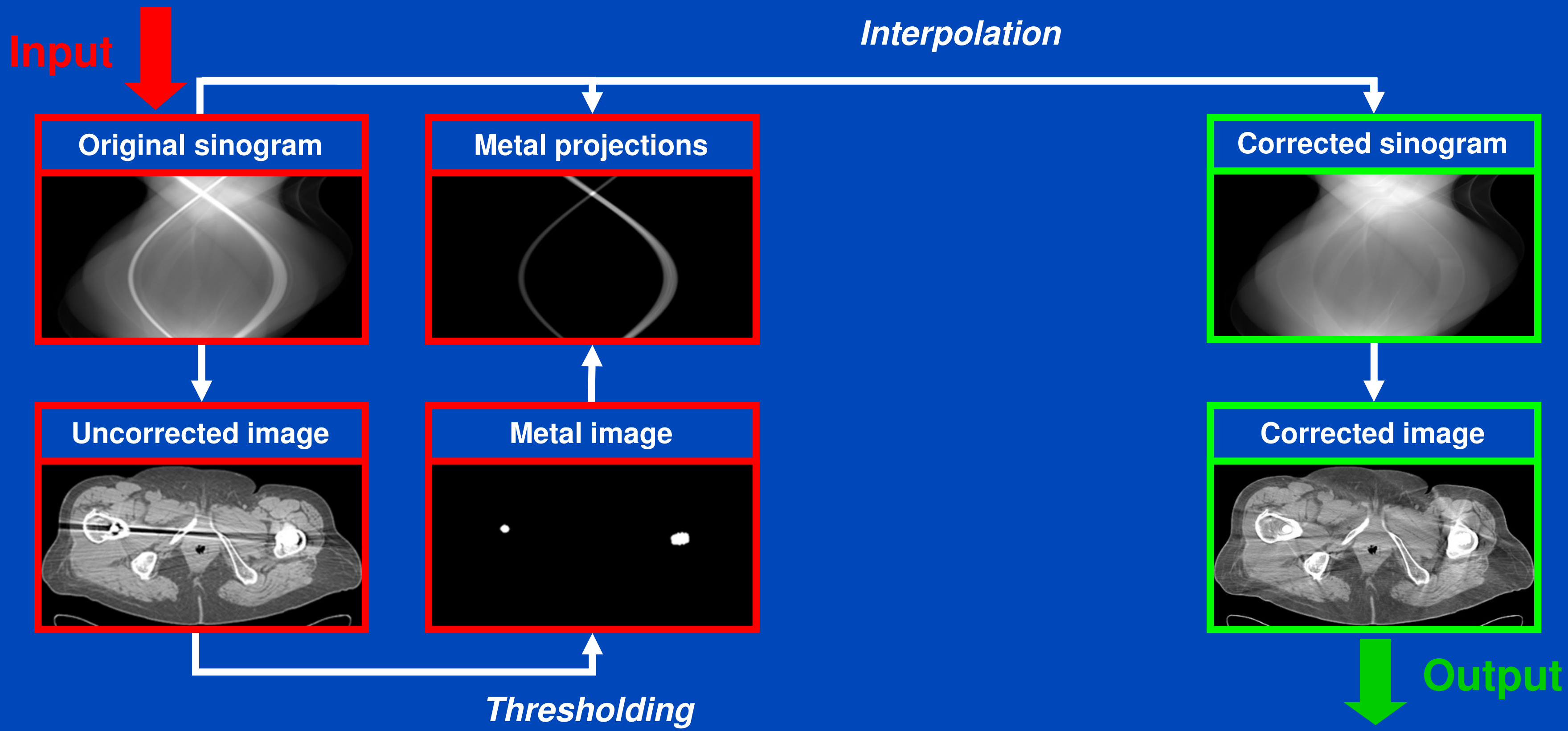

W. A. Kalender, R. Hebel, and J. Ebersberger, "Reduction of CT artifacts caused by metallic implants," Radiology 164(2): 576–577, 1987.

Normalized MAR (NMAR)

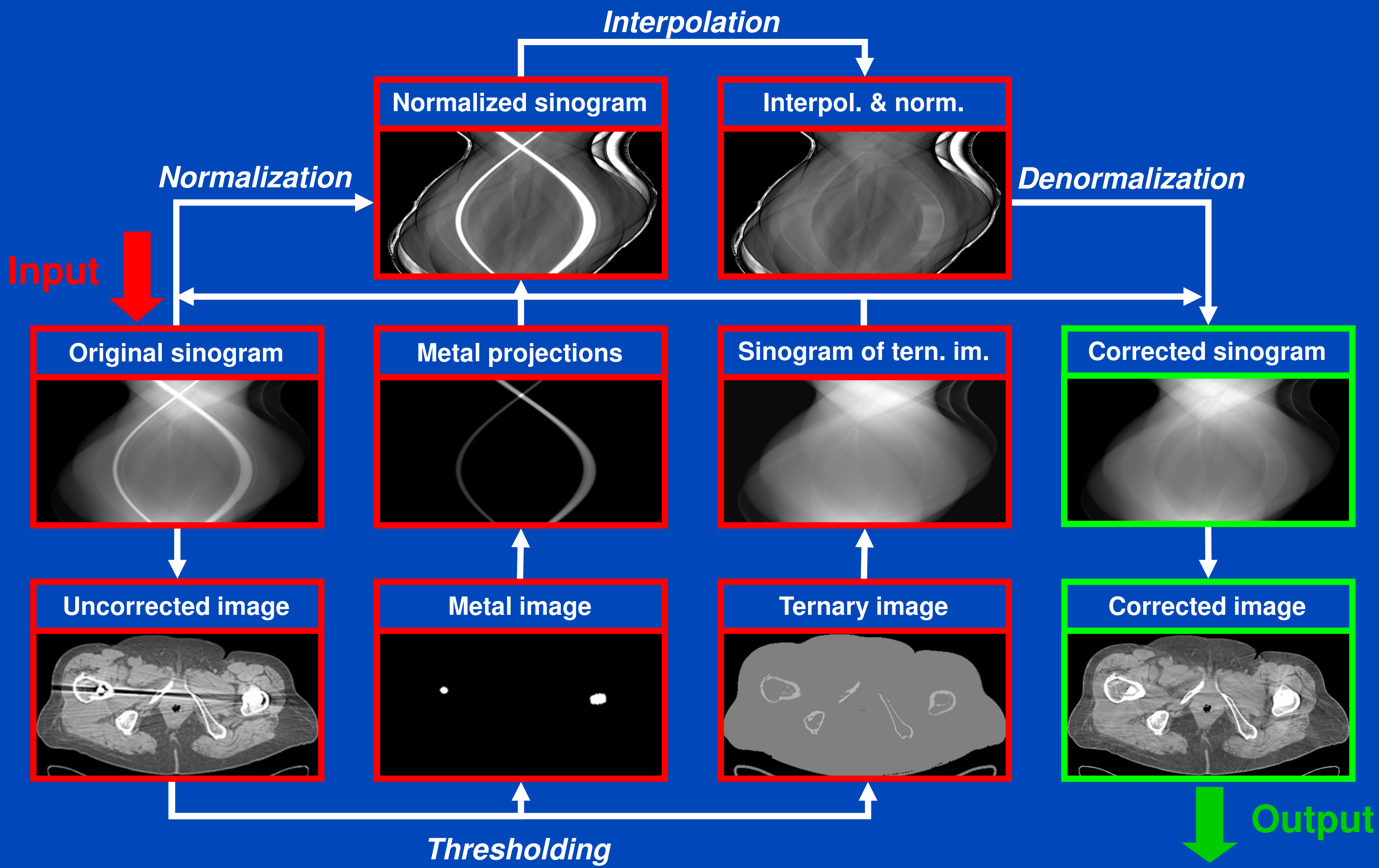

Meyer, Raupach, Lell, Schmidt, and Kachelrieß, "Normalized metal artifact reduction (NMAR) in computed tomography", Med. Phys. 37(10):5482-5493, 2012.

dkfz.

Results and Comparison: Patient Data

Uncorrected

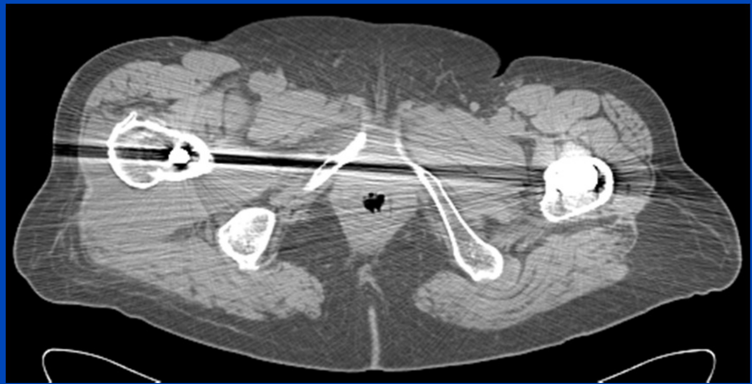

LIMAR

NMAR

Patient with hip implants, Sensation 16, 140 kV, (C = 0 HU, W = 500 HU)

Meyer, Raupach, Lell, Schmidt, and Kachelrieß, "Normalized metal artifact reduction (NMAR) in computed tomography", Med. Phys. 37(10):5482-5493, 2012.

Results and Comparison: Patient Data

Uncorrected

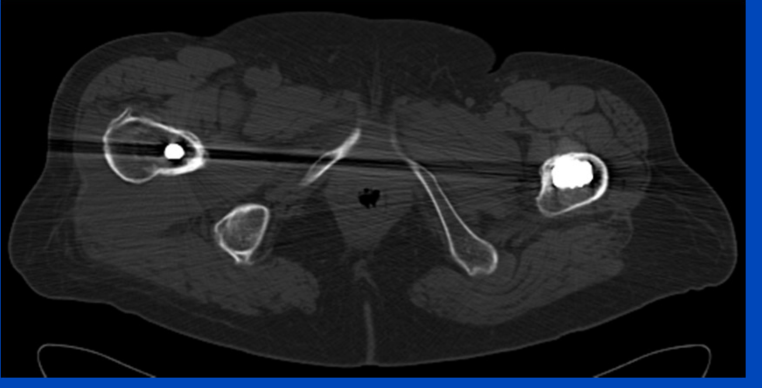

LIMAR

NMAR

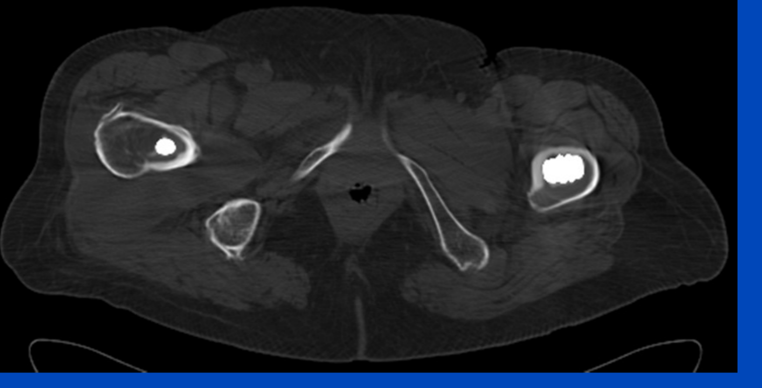

Patient with hip implants, Sensation 16, 140 kV, (C = 0 HU, W = 500 HU)

Results and Comparison: Patient Data

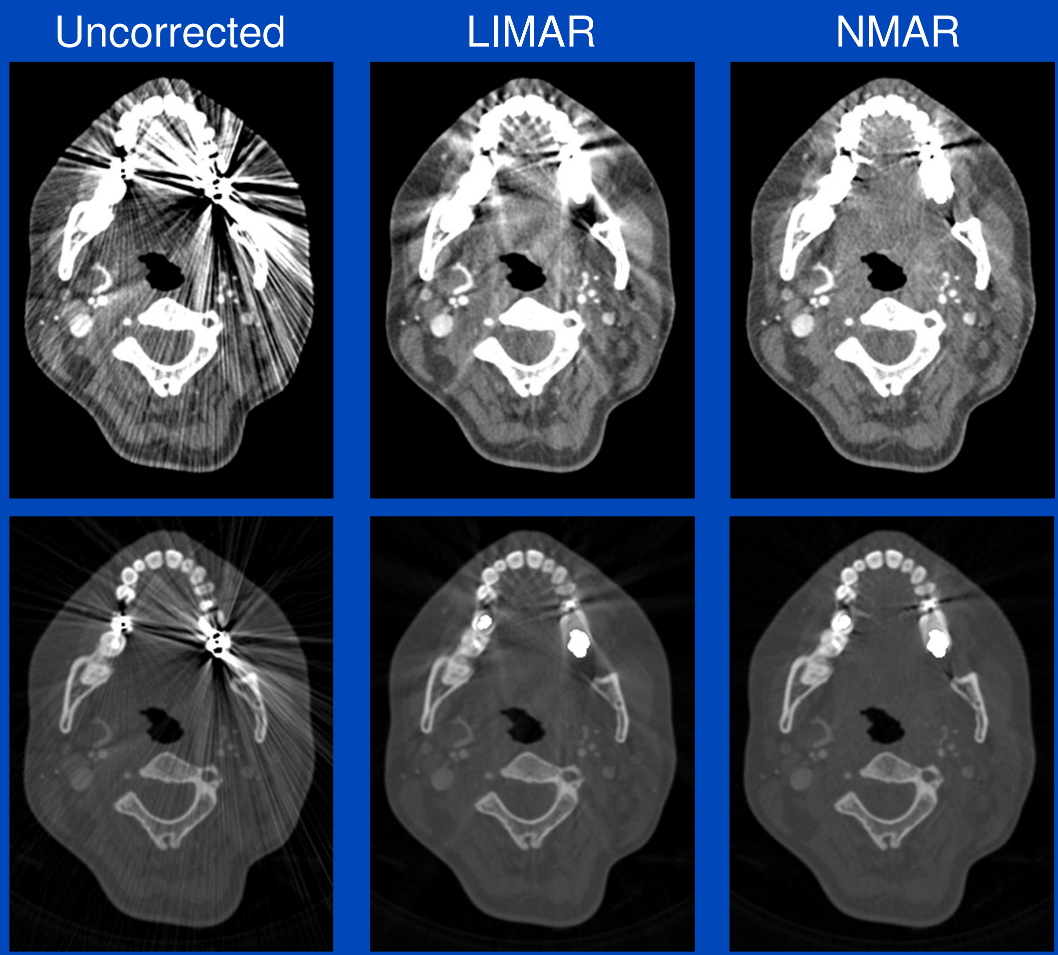

Patient dental fillings, slice 110, Somatom Definition Flash, pitch 0.9.
Top row: (C = 100 HU, W = 750 HU). Bottom row: (C = 1000 HU, W = 4000 HU)

FSMAR: Scheme

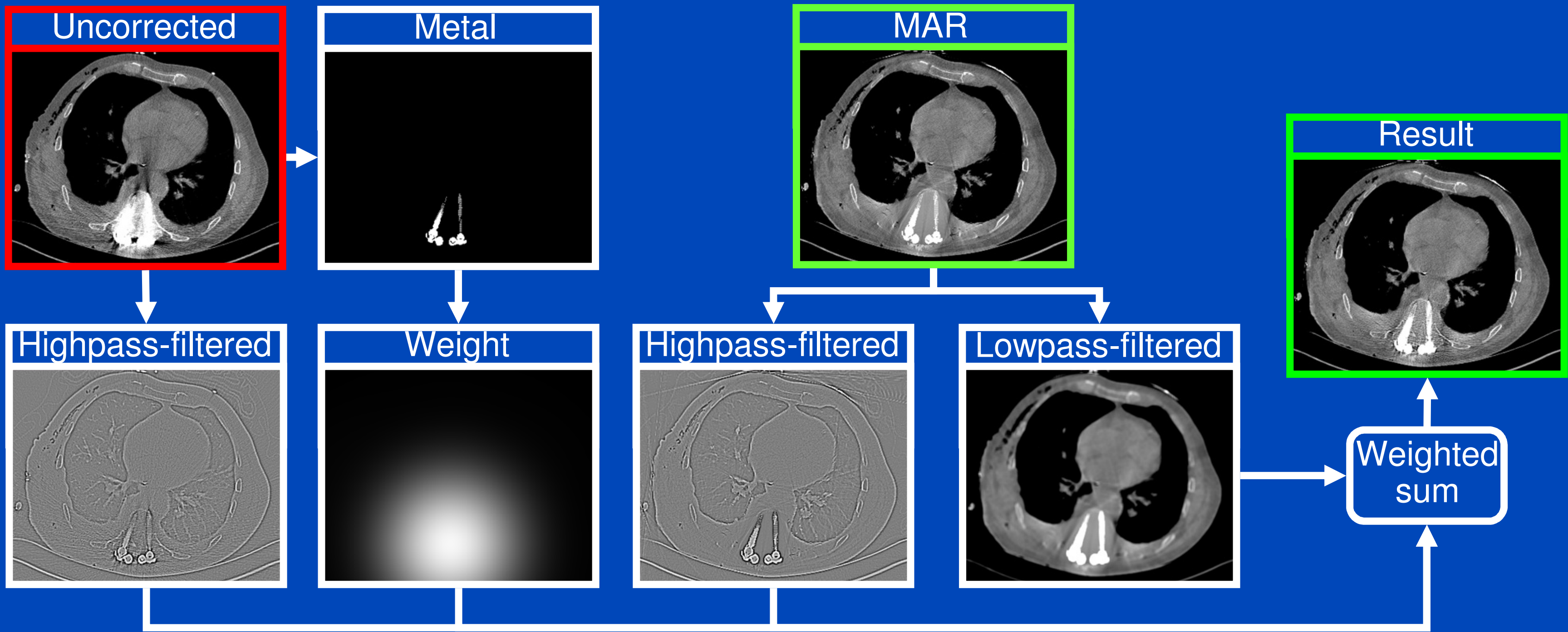

Meyer, Raupach, Lell, Schmidt, and Kachelrieß, "Frequency split metal artifact reduction (FSMAR) in computed tomography", Med. Phys. 39(4):1904-1916, 2012.

FSMAR: Results

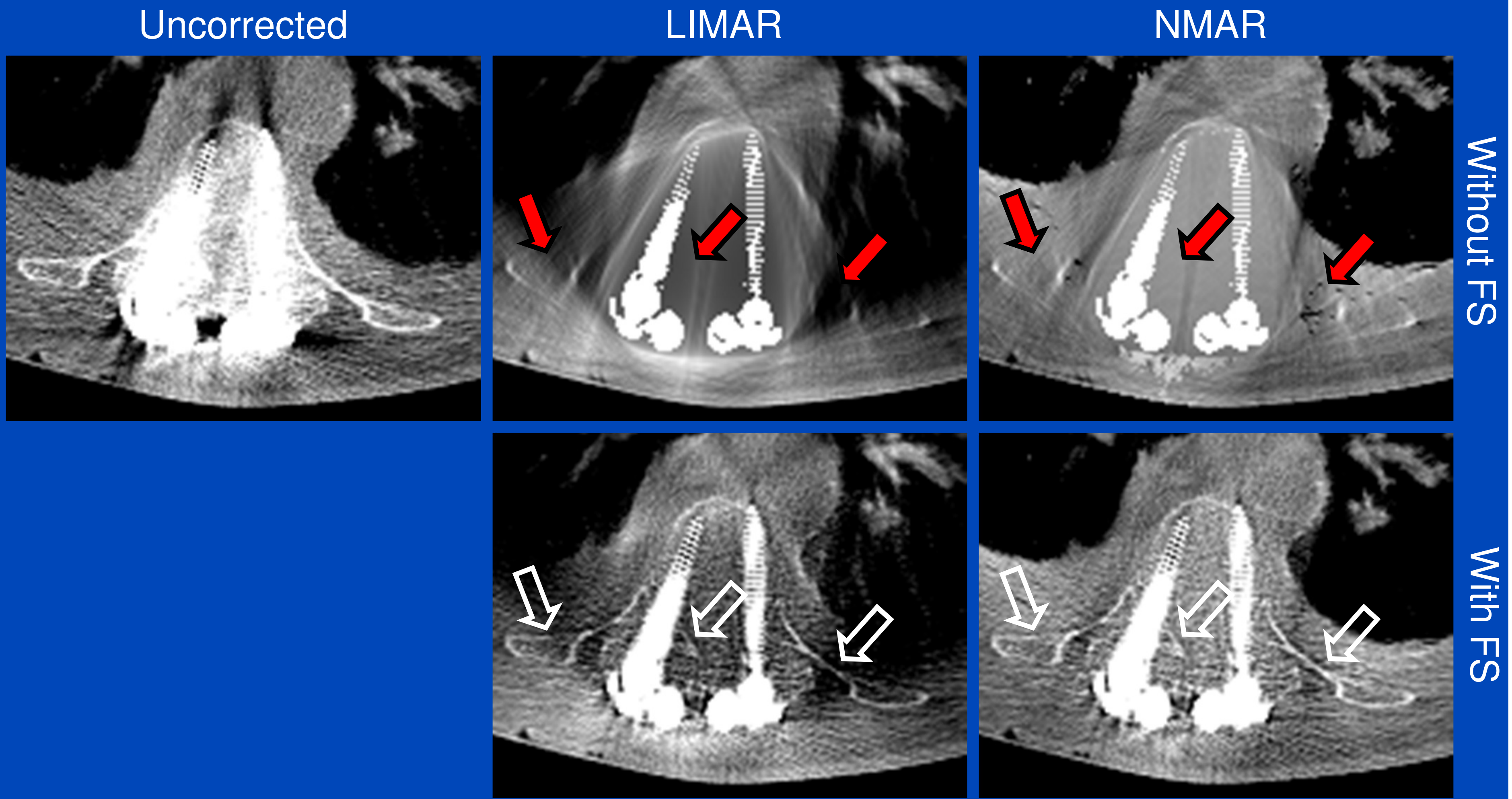

Patient with spine fixation, Somatom Definition, (C=100/W=1000).

Meyer, Raupach, Lell, Schmidt, and Kachelrieß, "Frequency split metal artifact reduction (FSMAR) in computed tomography", Med. Phys. 39(4):1904-1916, 2012.

dkfz.

NMAR: Results

Uncorrected

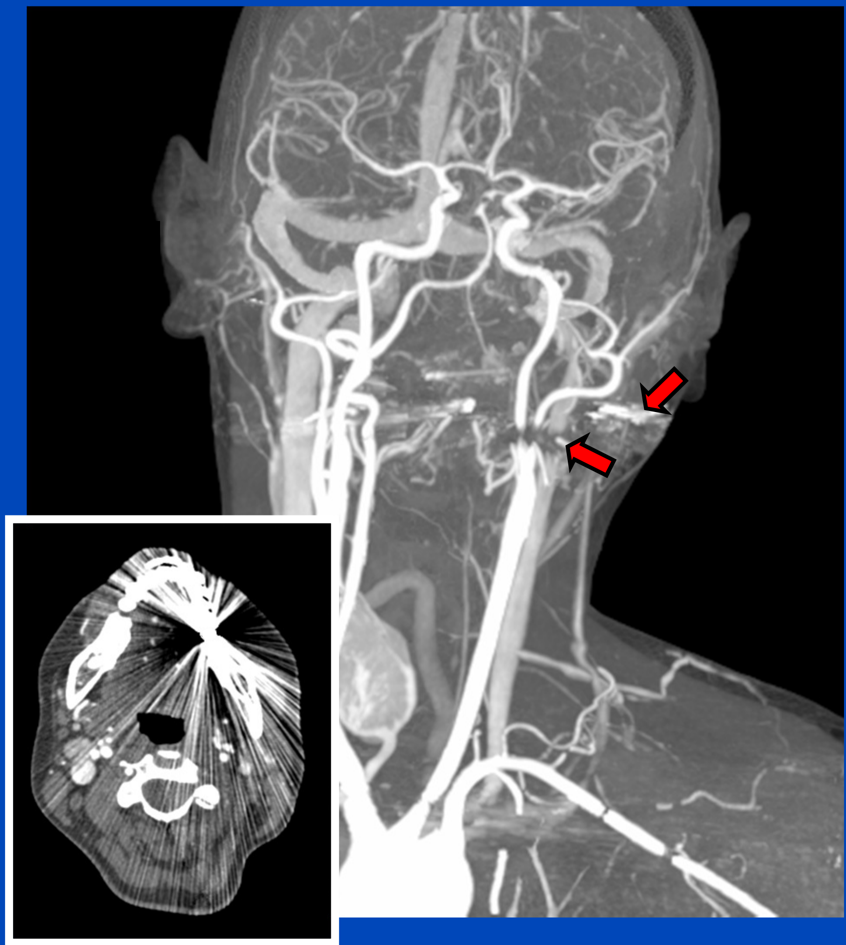

NMAR

Bone removal (with scanner software), (C=40/W=500).

DECT and Pseudo Monochromatic Imaging

Pseudo monochromatic imaging is a linear combination of DECT f_L and f_H: $f_\alpha = (1-\alpha)\, f_\mathrm{L} + \alpha\, f_\mathrm{H}$

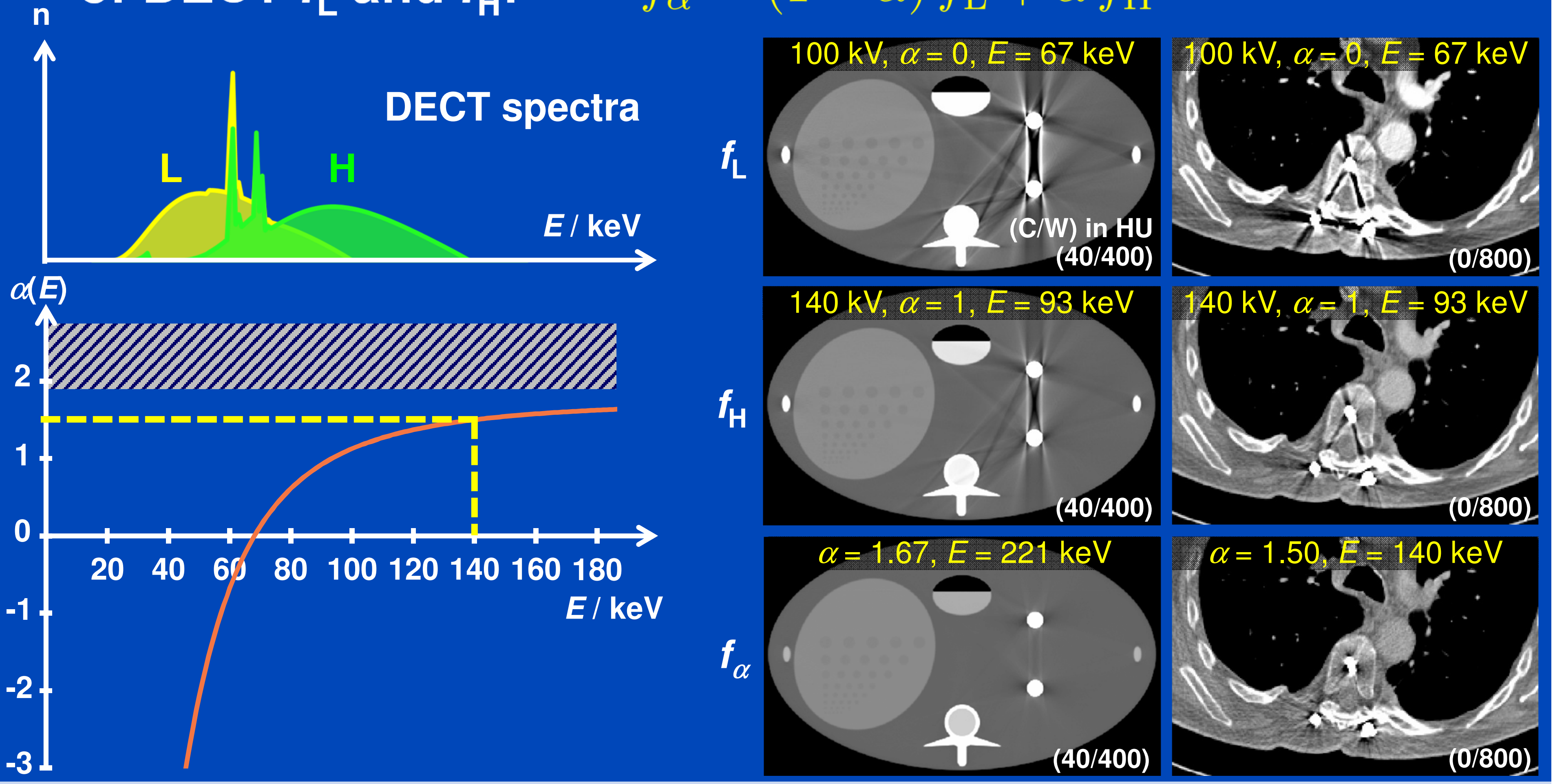

dkfz.

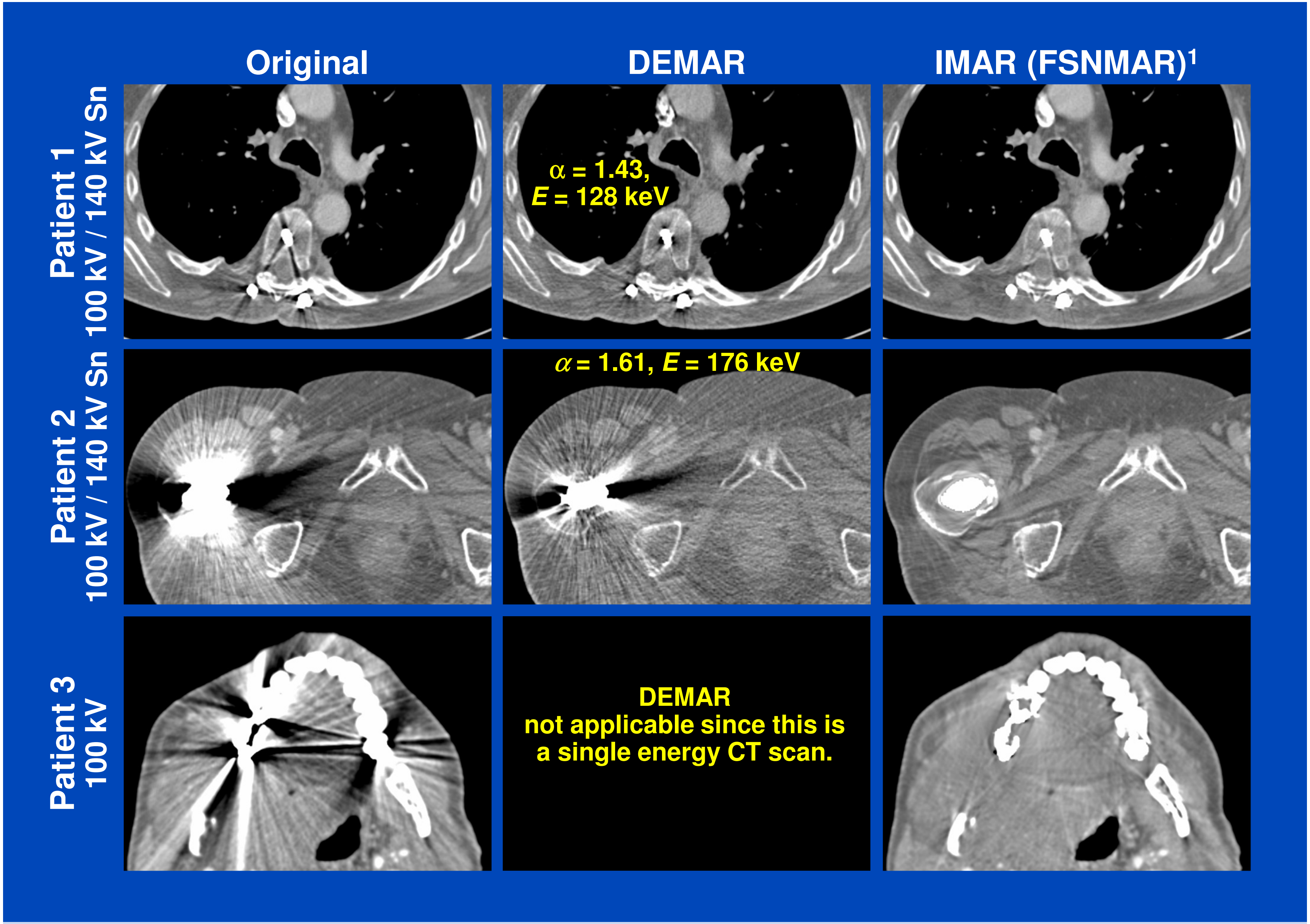

[1]Iterative metal artifact reduction (IMAR) is the Siemens product implementation of FSNMAR.

Further Reading

- Maik Stille, Matthias Kleine, Julian Haegele, Jörg Barkhausen, and Thorsten M. Buzug. Augmented Likelihood Image Reconstruction. IEEE Transactions on Medical Imaging 35(1), 158–173, July 2015.
- Webster J. Stayman, Yoshito Otake, Jerry L. Prince, Jay A. Khanna, and Jeffery H. Siewerdsen. Model-based tomographic reconstruction of objects containing known components. IEEE Transactions on Medical Imaging 31(10), 1837–1848, October 2012.
- Yi Zhang, Yifei Pu, Jin-Rong Hu, Yan Liu, Ji-Liu Zhou. A new CT metal artifacts reduction algorithm based on fractional-order sinogram inpainting. J Xray Sci Technol. 19(3), 373-84, January 2011.

Cone-Beam Artifacts

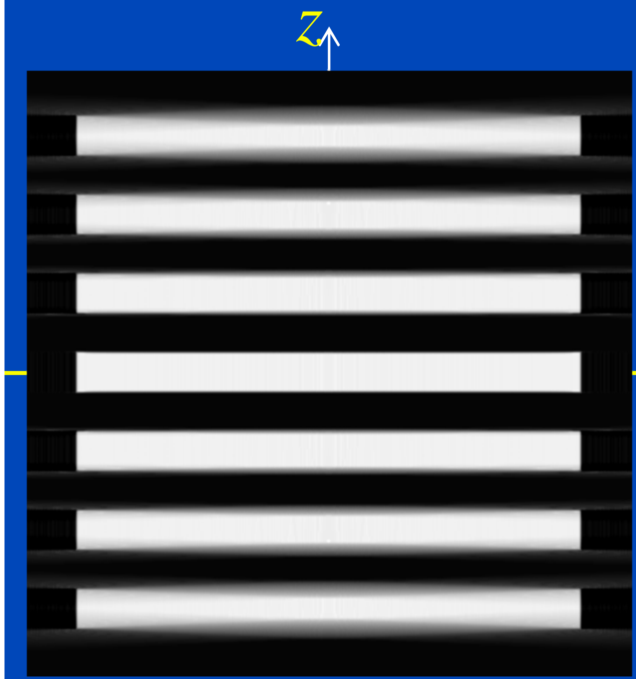

Cone-angle Γ = 6°

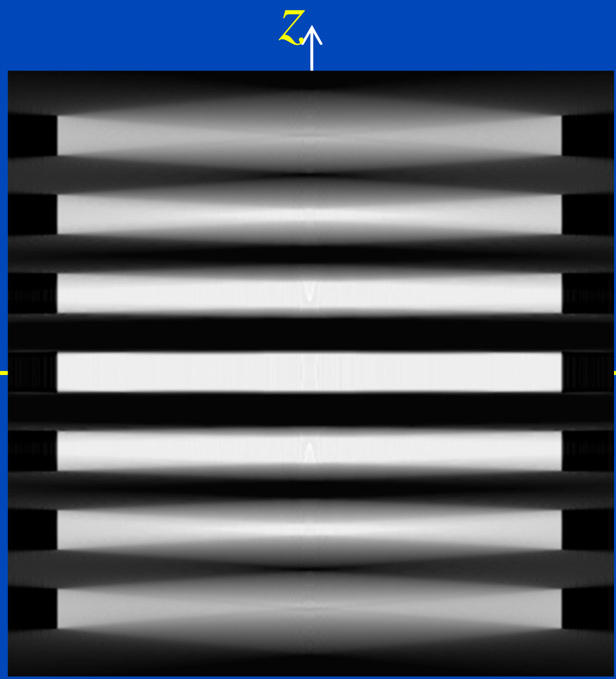

Cone-angle Γ = 14°

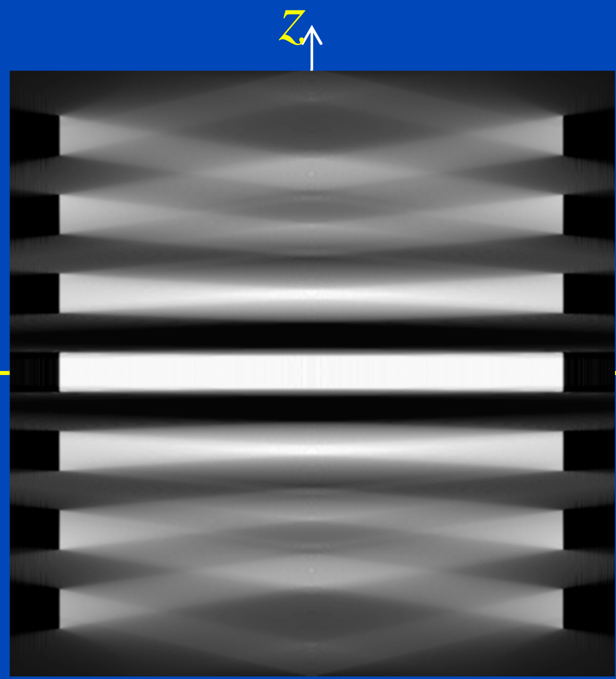

Cone-angle Γ = 28°

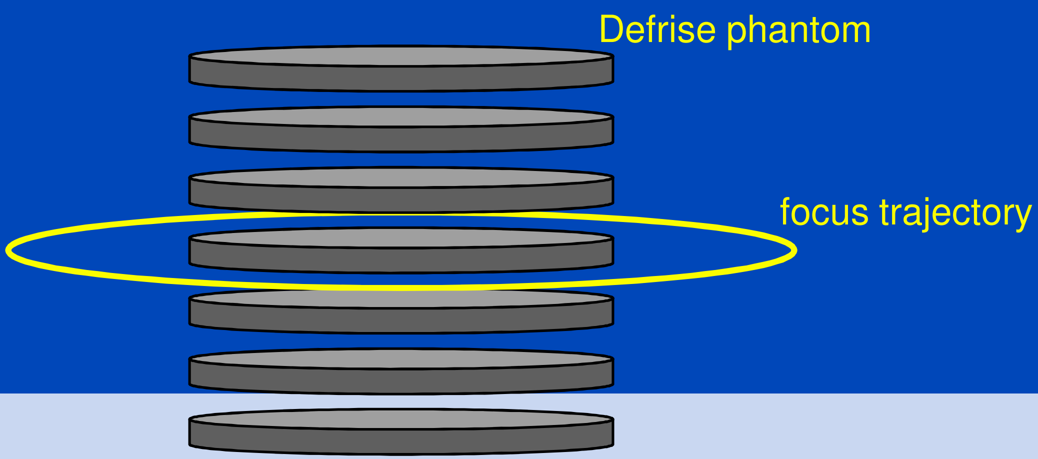

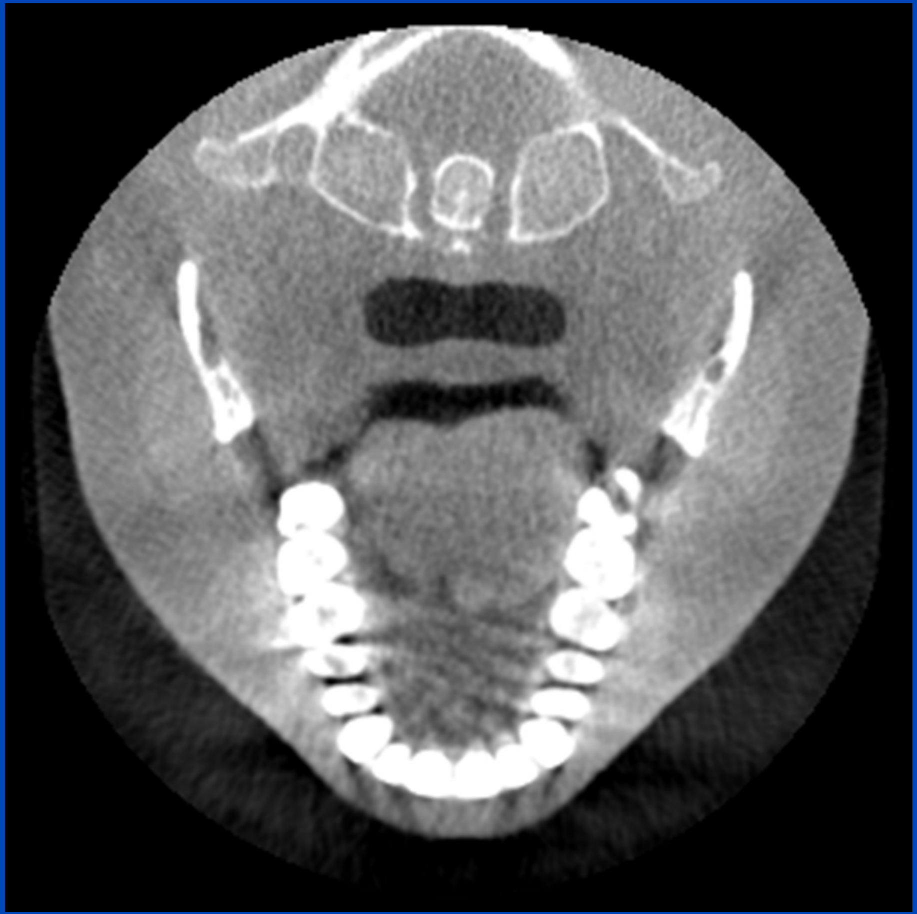

Cone-Beam Artifact Correction Method

1. **Reconstruct an image *$f^{(0)}$* from the rawdata *p*, e.g. by performing a filtered backprojection X^{-1} :**

$$f^{(0)} = \mathsf{X}^{-1} p$$

2. **Apply a segmentation S to the reconstructed volume *$f^{(0)}$* :**

$$f_S = S f^{(0)}$$ ⟵ ***prior knowledge enters here***

3. **Perform a forward projection and reconstruction of *f_S*:**

$$f^{(1)} = \mathsf{X}^{-1} \mathsf{X} f_S$$

4. **Subtract the volume *f_S* from the resulting volume *$f^{(1)}$* :**

$$f_{\mathrm{artifacts}} = f_S - f^{(1)}$$

5. **Remove the artifacts *$f_{artifacts}$* from the original volume *$f^{(0)}$* :**

$$f_{\mathrm{final}} = f^{(0)} - f_{\mathrm{artifacts}}$$

$$f_{\mathrm{final}} = f^{(0)} - (f_S - \mathsf{X}^{-1} \mathsf{X} f_S)$$

J. Hsieh, "A two-pass algorithm for cone beam reconstruction," in *Proceedings of the SPIE Medical Imaging Conference*, 2000, Vol. 3979, pp.533–540.

Cone-Beam Artifact Correction Method

- The method is less efficient without the segmentation step (but still shows positive effects)
- It is less efficient without data redundancies, e.g. in case of
  - short scans
  - shifted detector scans
- We demonstrate issues measuring a skull phantom in shifted detector geometry with a (simulated) small FOM (data truncation) flat detector CT.

Weighting and Detruncation

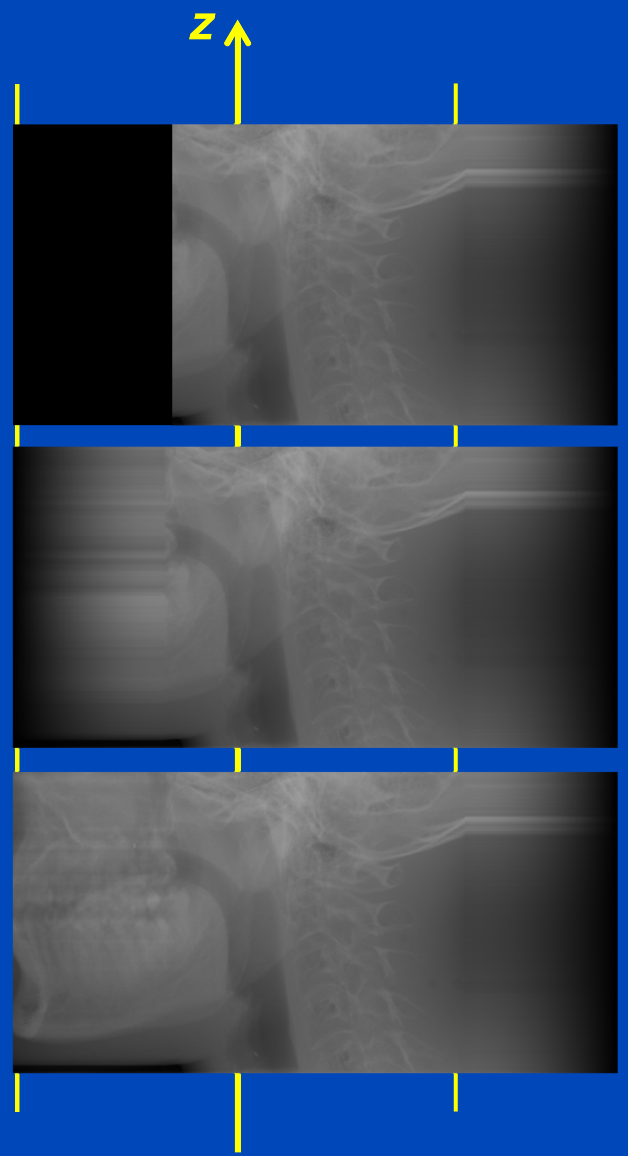

Rawdata for preweighted
shifted detector FDK

Rawdata for postweighted
shifted detector FDK (simple extrapolation)

Rawdata for postweighted
shifted detector FDK (super extrapolation)

C = 3; W = 6

Note: Post weighting shifted detector recon is not exact in the mid-plane. But it may have favourable artifact behaviour.

FDK Preweight

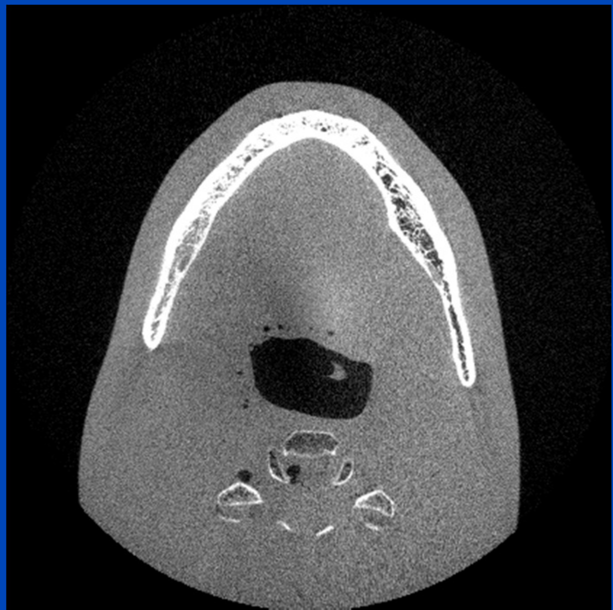

shifted detector scan 360°

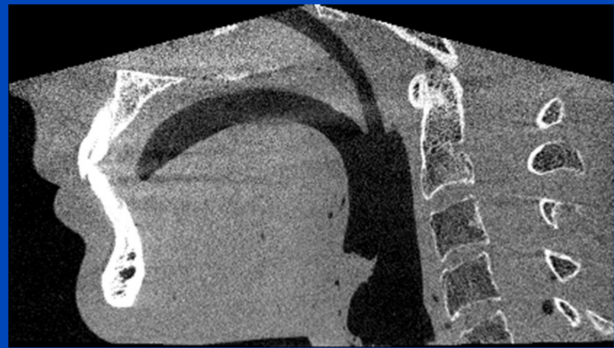

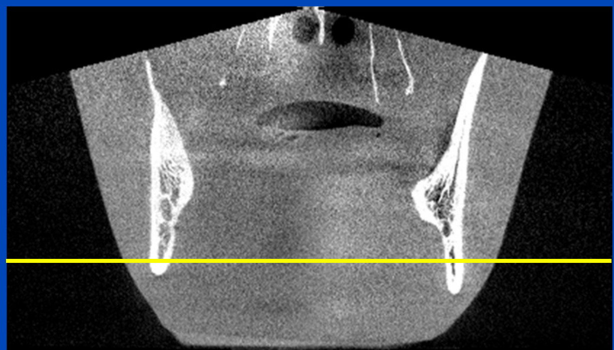

Midplane

C = 0 HU; W = 2000 HU

FDK Preweight
Cone-Beam Corrected

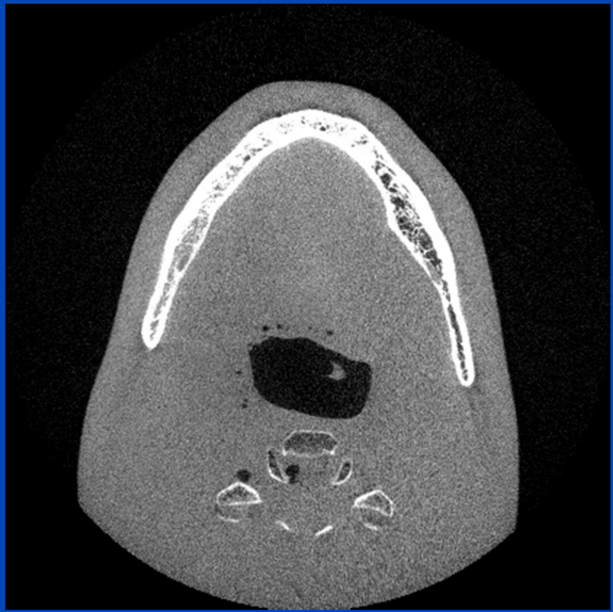

shifted detector scan 360°

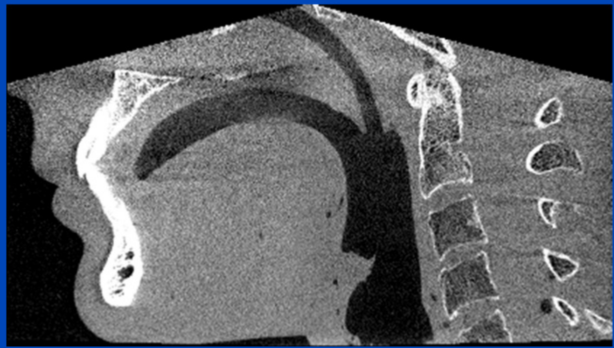

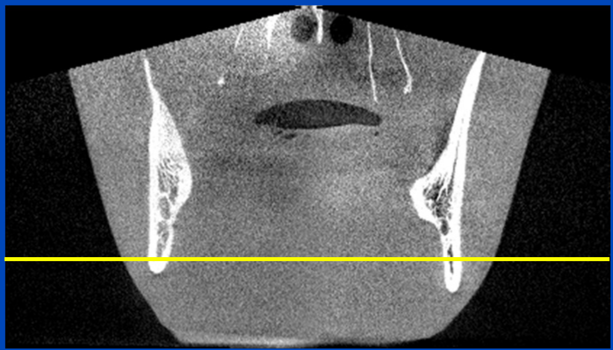

Midplane

C = 0 HU; W = 2000 HU

dkfz.

FDK Preweight

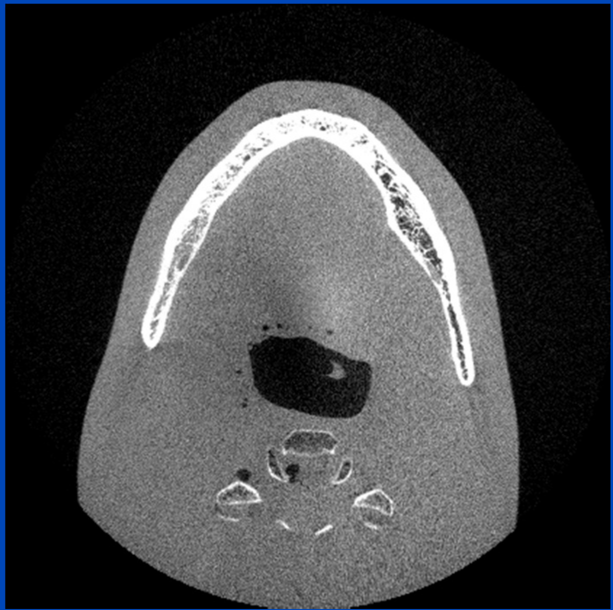

shifted detector scan 360°

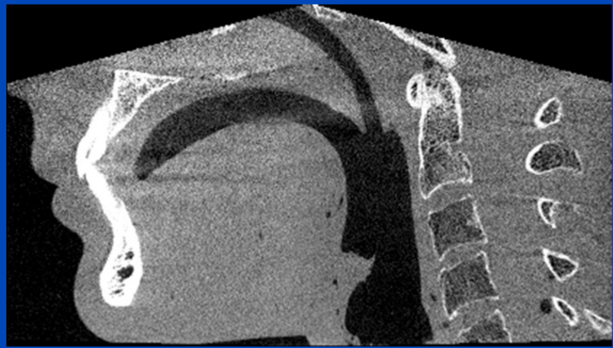

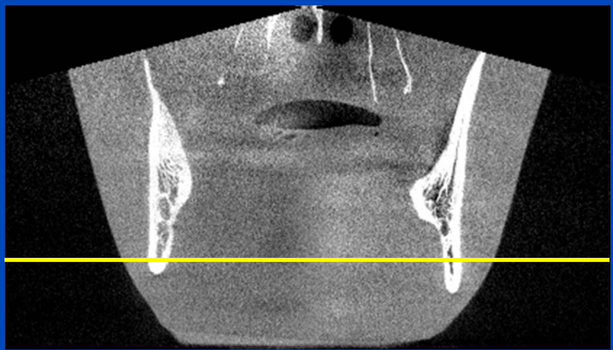

Midplane

C = 0 HU; W = 2000 HU

FDK Postweight

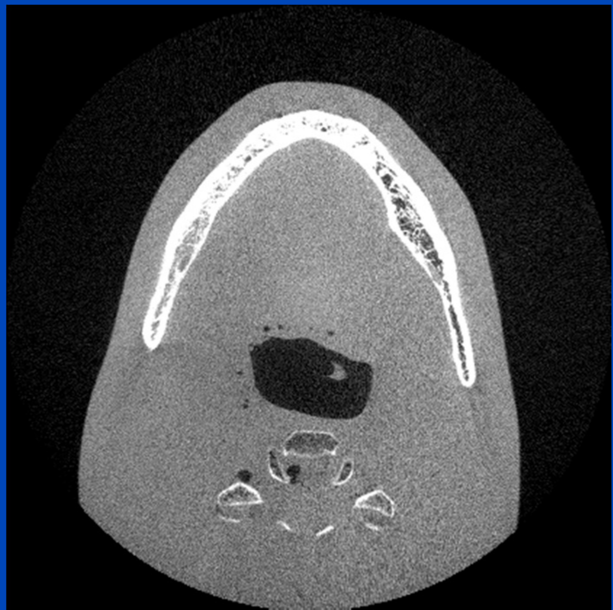

shifted detector scan 360°

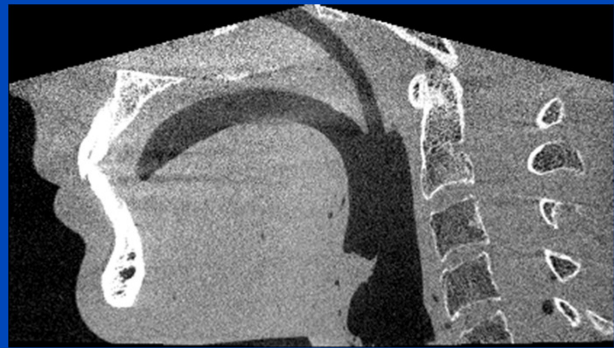

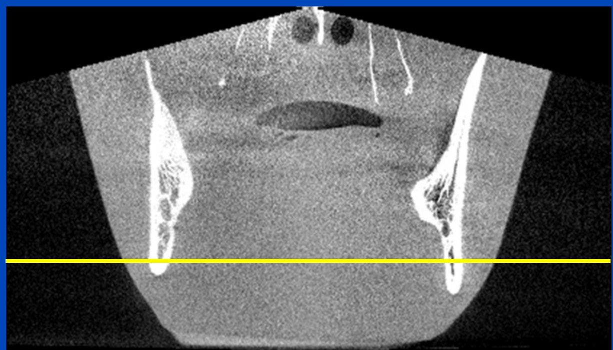

Midplane

C = 0 HU; W = 2000 HU

FDK Postweight Super Extrapolation

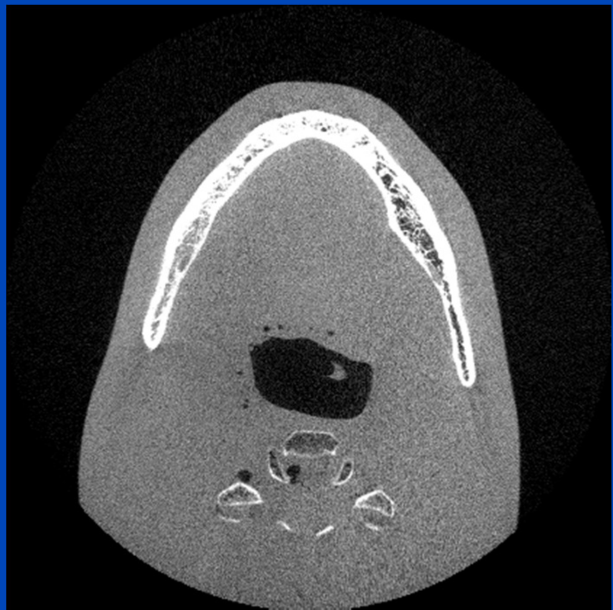

shifted detector scan 360°

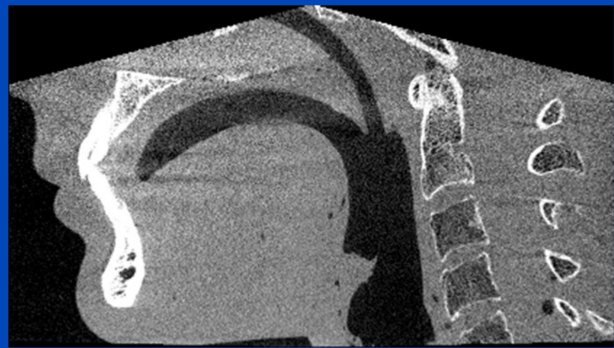

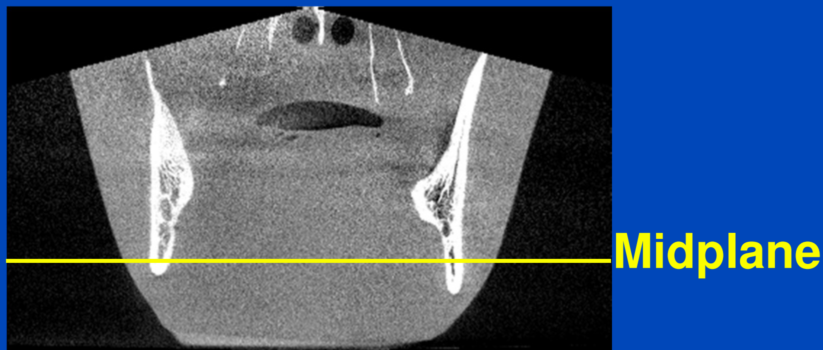

C = 0 HU; W = 2000 HU

FDK Preweight
Cone-Beam Corrected

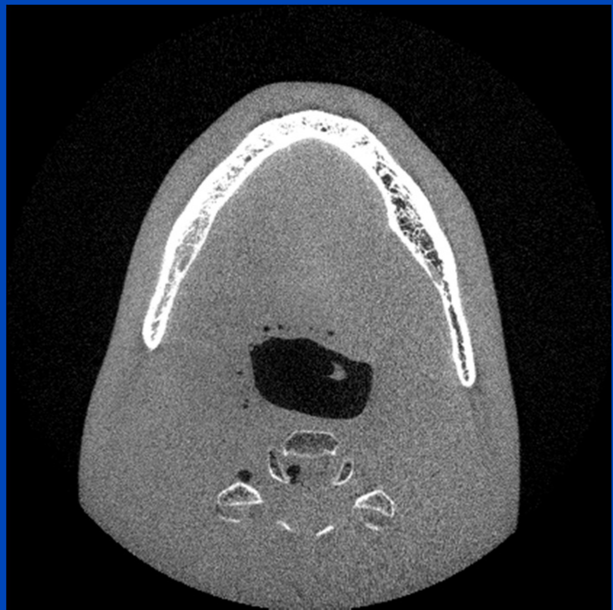

shifted detector scan 360°

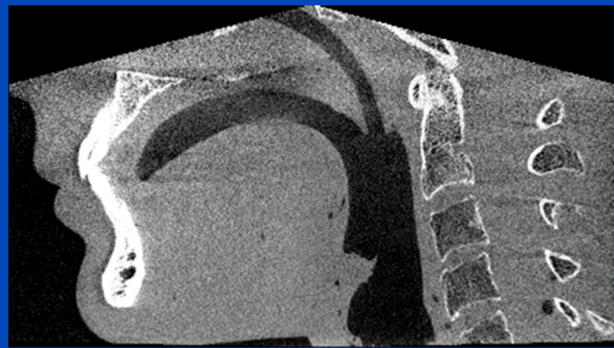

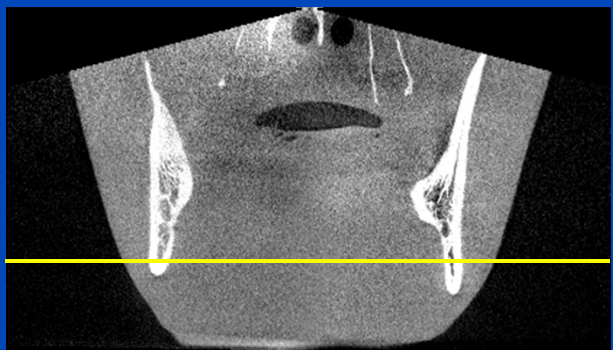

Midplane

C = 0 HU; W = 2000 HU

FDK Postweight Super Detruncation Cone-Beam Corrected

shifted detector scan 360°

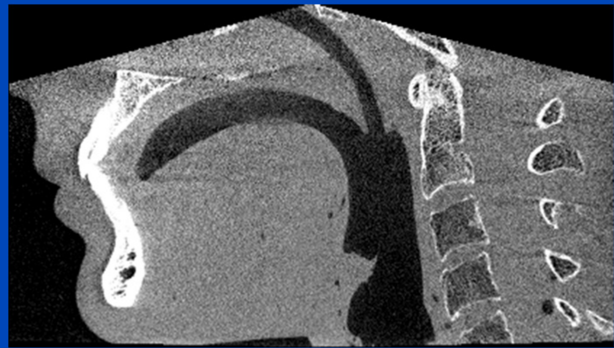

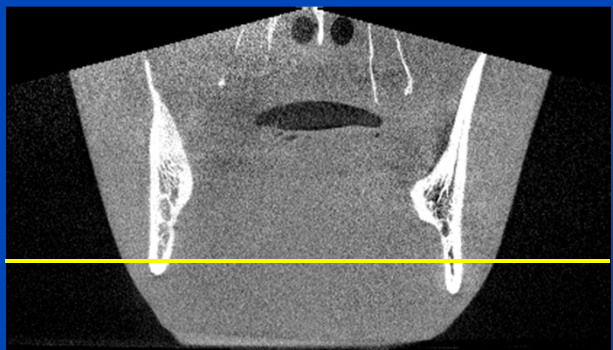

Midplane

C = 0 HU; W = 2000 HU

Further Reading

- Dirk Schäfer, Michael Grass, and Peter van de Haar. FBP and BPF reconstruction methods for circular X-ray tomography with off-center detector. Med. Phys. 38(7): S85-S94, July 2011.
- Jed D. Pack, Kai Zeng, Adam Budde, Zhye Yin, Bruno De Man. Mitigating cone-beam artifacts via shift-variant data usage for large cone-angle scans. Conference Program of the 3rd International Conference on Image Formation in X-Ray Computed Tomography:307-310, June 2014.

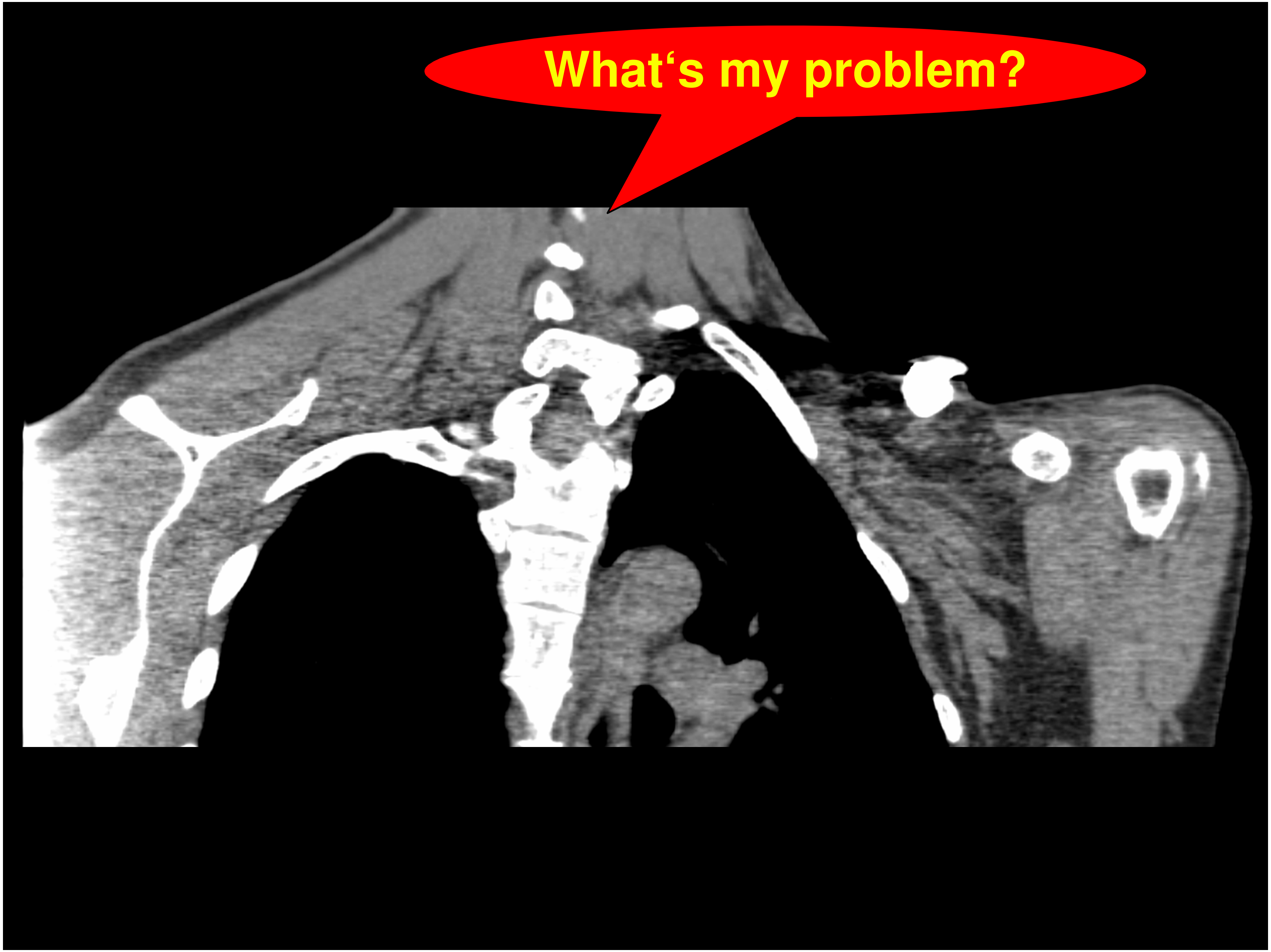
What‘s my problem?

Adaptive Detruncation Method (ADT)

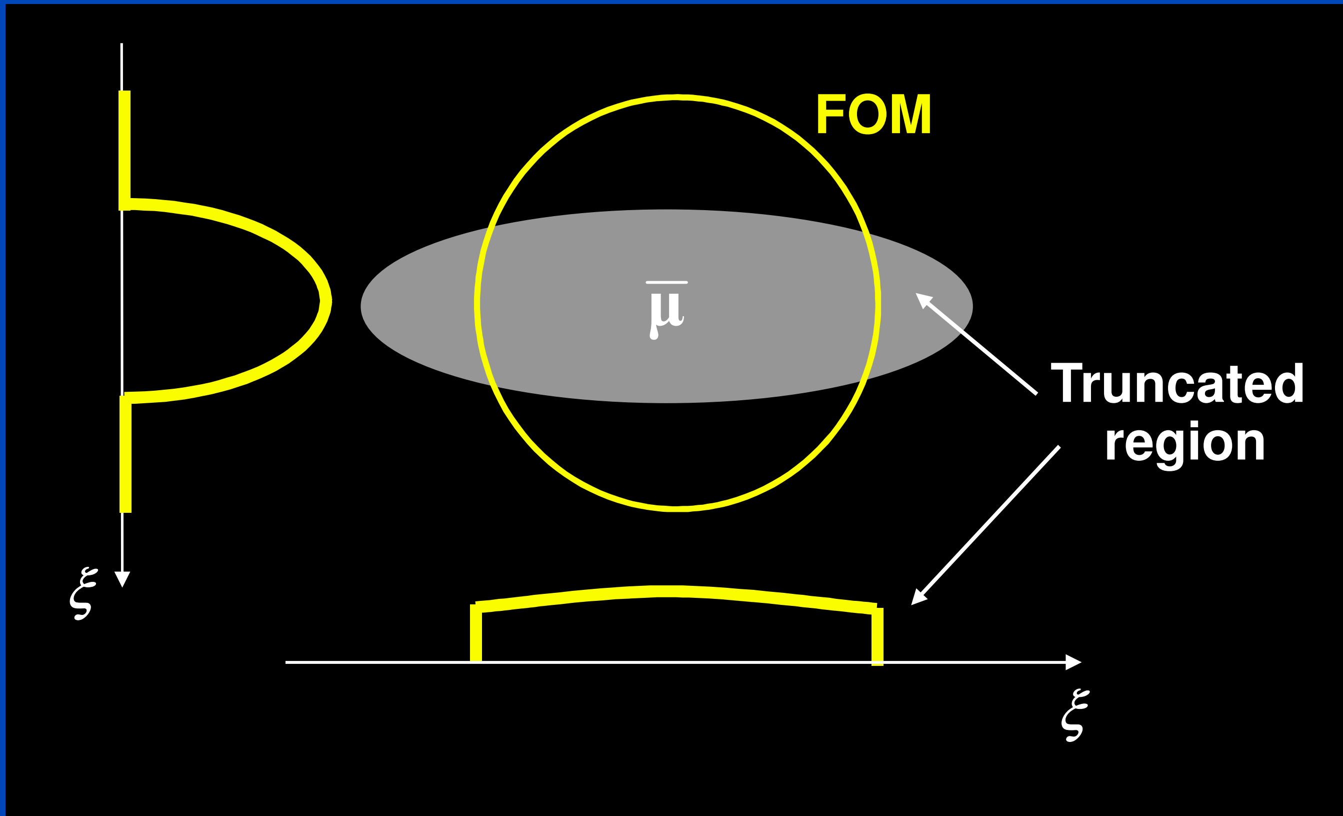

K. Sourbelle, M. Kachelrieß, and W.A. Kalender, “Reconstruction from truncated projections in CT using adaptive detruncation,” Eur Radiol 15:1008–1014, 2005.

dkfz.

Adaptive Detruncation Method (ADT)

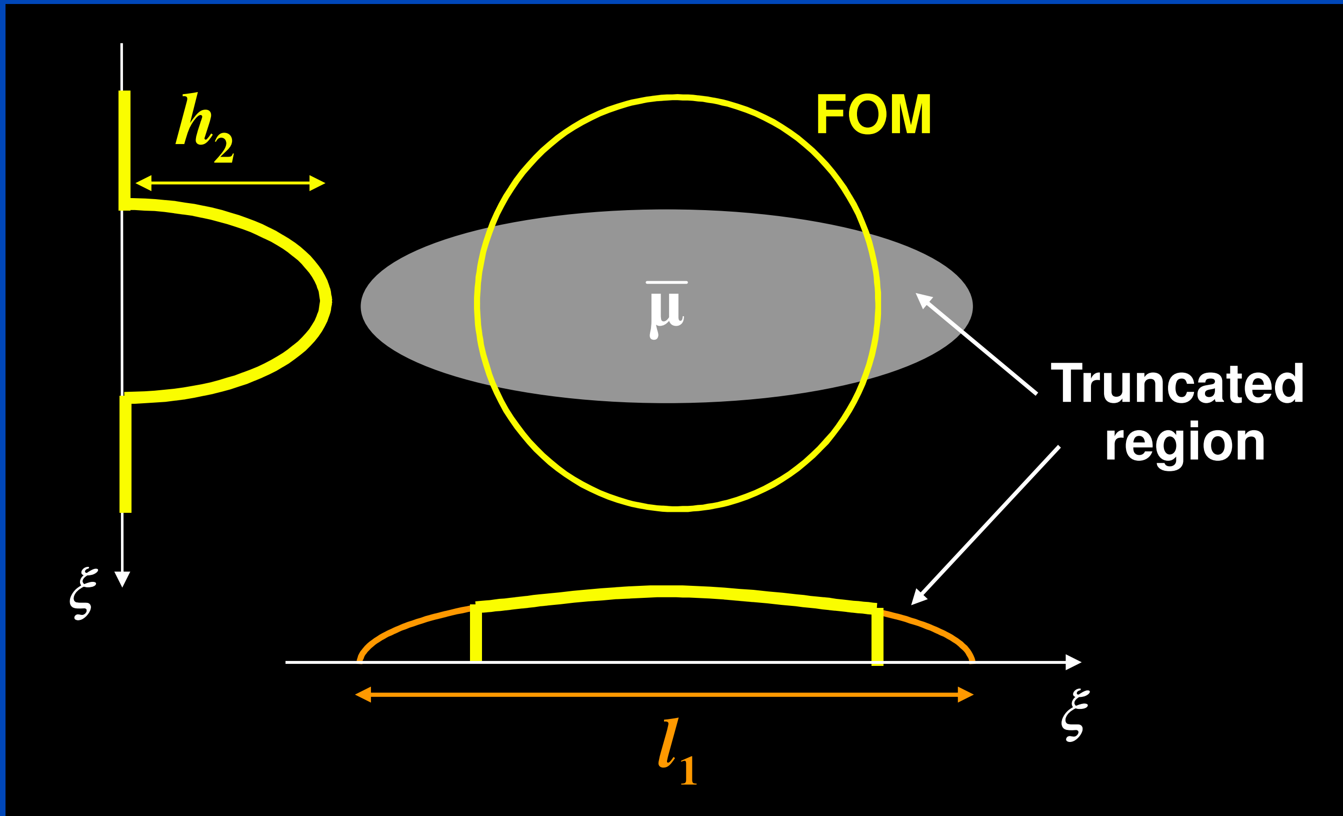

Data consistency

$$l_1 = h_2 / \bar{\mu}$$

$$A_1 = A_2$$

Smooth extrapolation

$$\sqrt{a\xi^2 + b\xi + c}$$

K. Sourbelle, M. Kachelrieß, and W.A. Kalender, "Reconstruction from truncated projections in CT using adaptive detruncation," Eur Radiol 15:1008–1014, 2005.

Adaptive Detruncation Method (ADT)

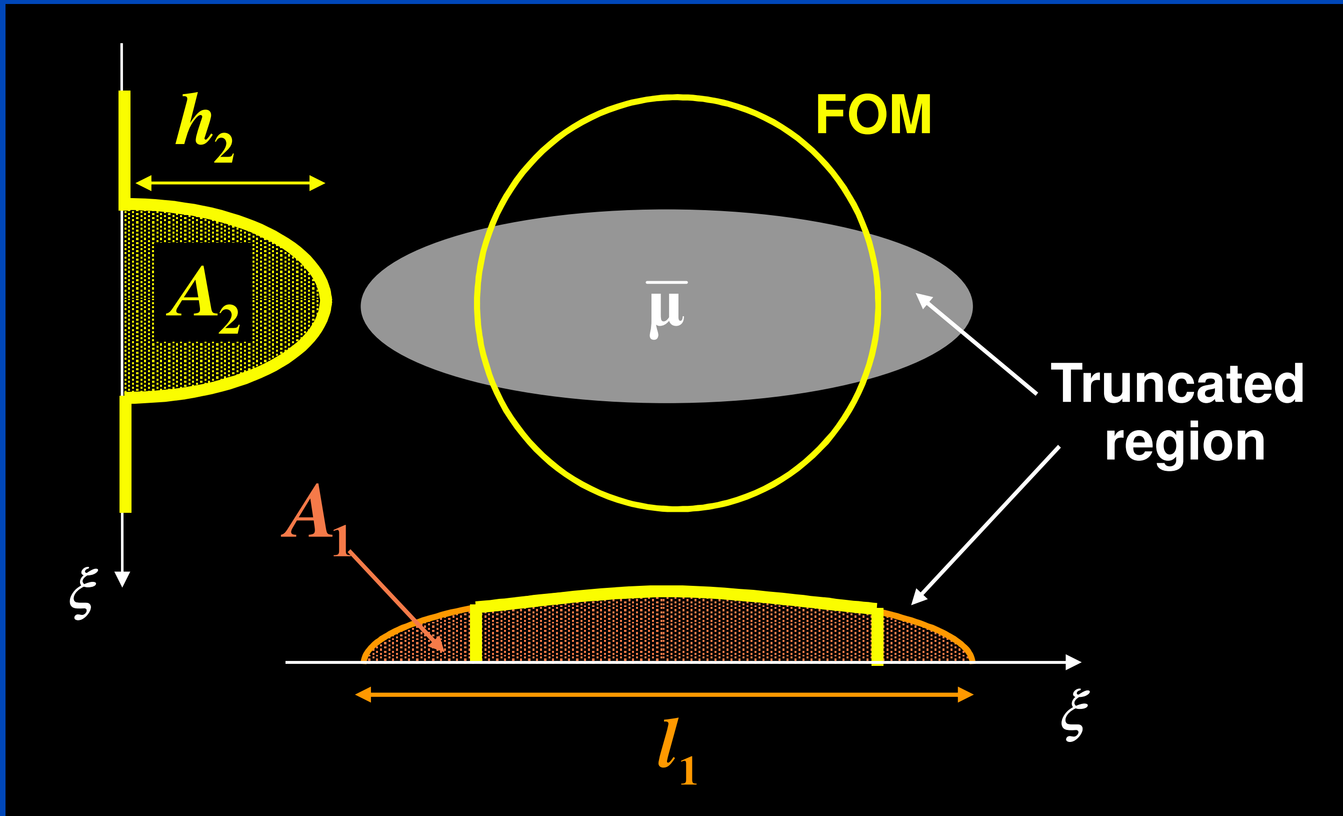

Data consistency

$$l_1 = h_2/\bar{\mu}$$

$$A_1 = A_2$$

Smooth extrapolation

$$\sqrt{a\xi^2 + b\xi + c}$$

K. Sourbelle, M. Kachelrieß, and W.A. Kalender, "Reconstruction from truncated projections in CT using adaptive detruncation," Eur Radiol 15:1008–1014, 2005.

Example : 2 × 100 suppressed columns

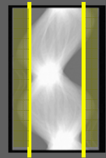

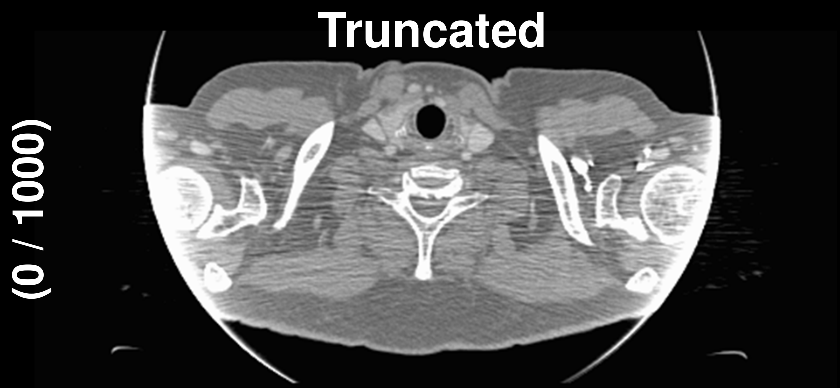

Example :
2×100 suppressed columns

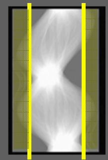

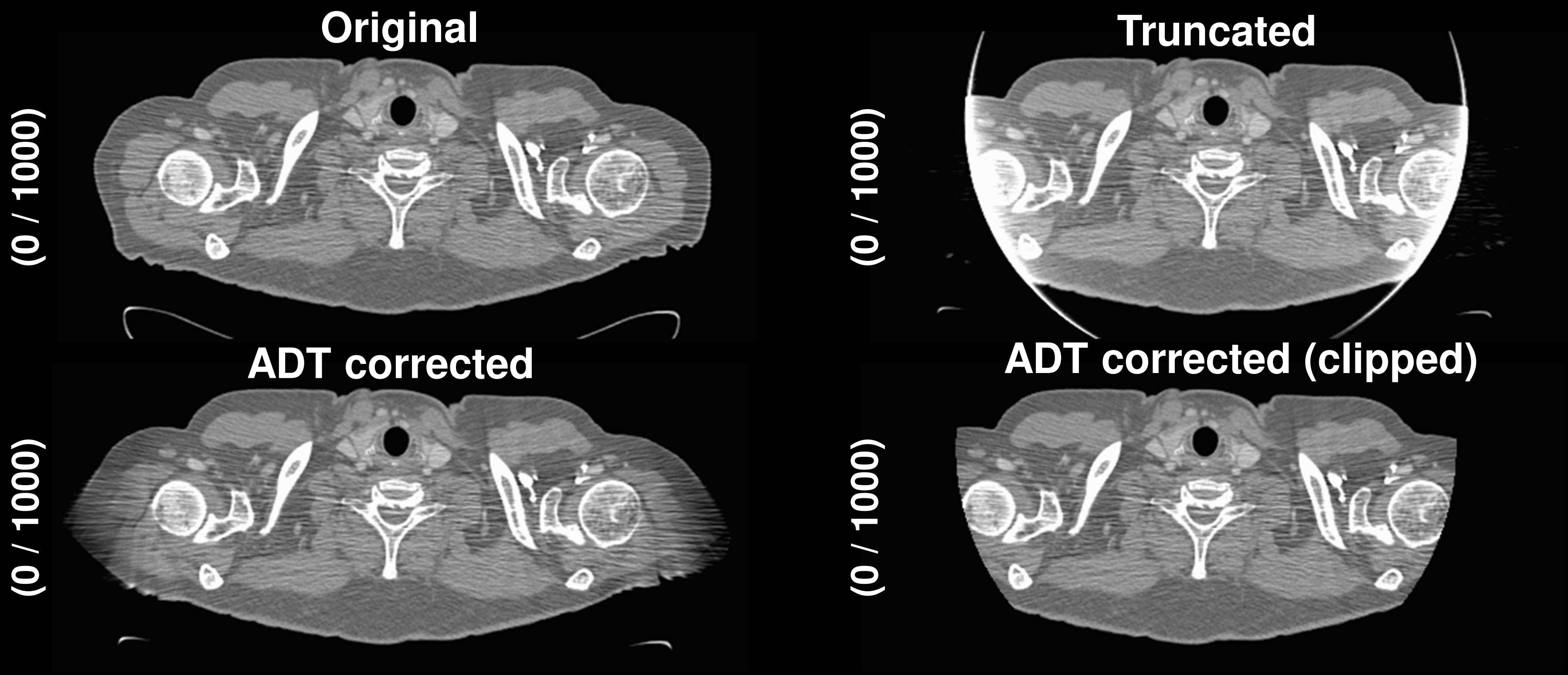

Example :
2 × 100 suppressed columns

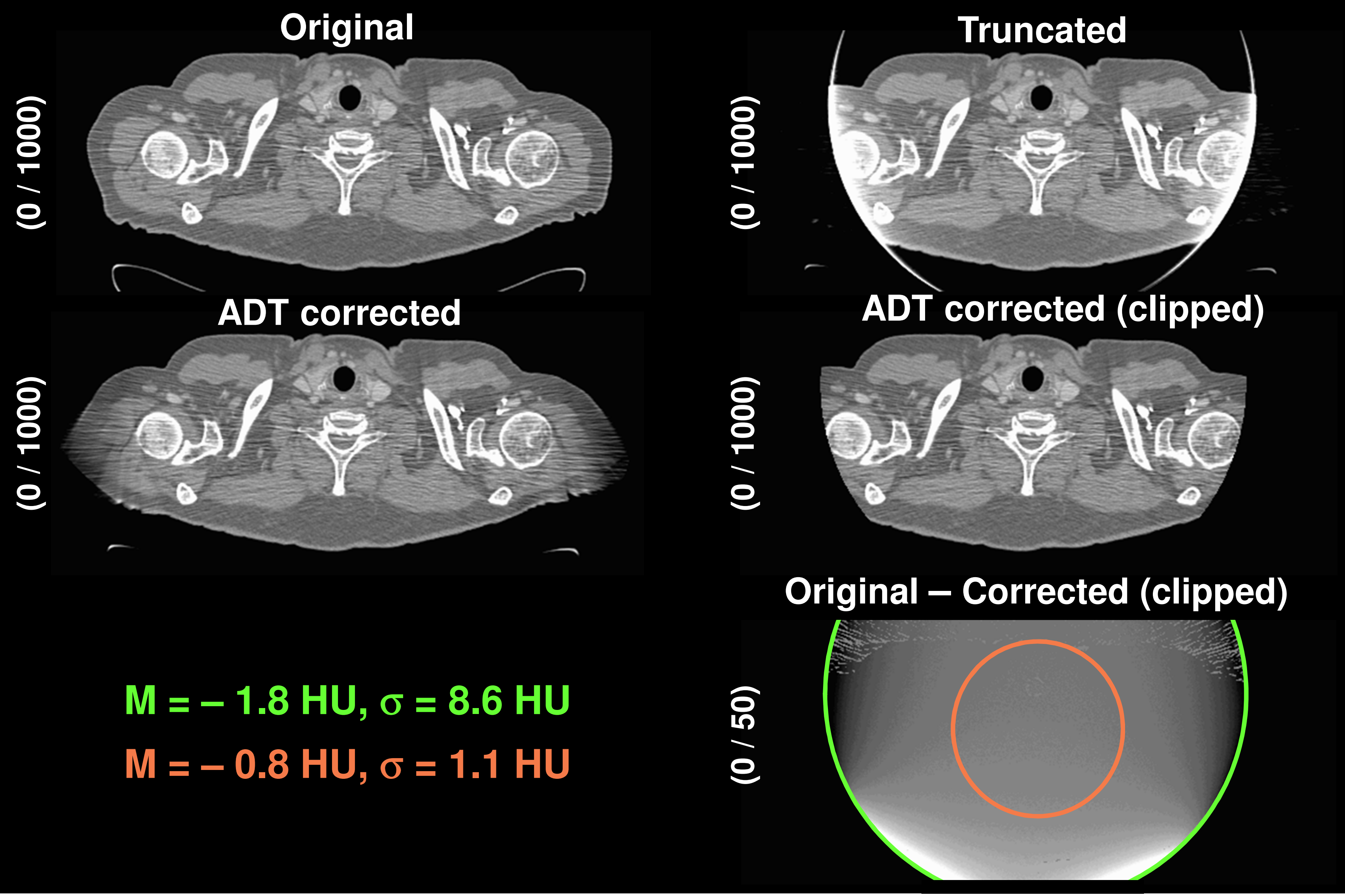

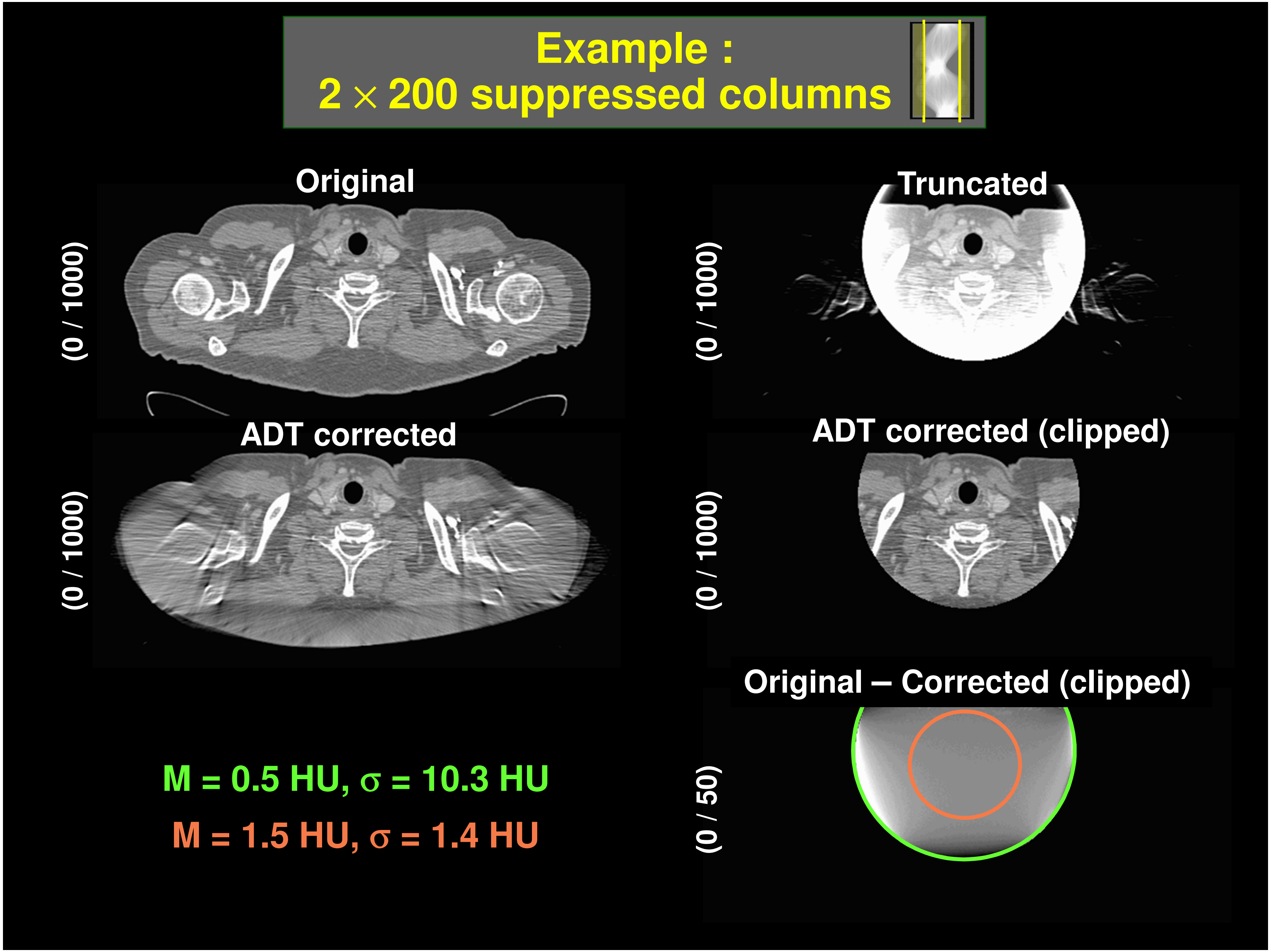
Example :
2 × 200 suppressed columns
Original
(0 / 1000)
Truncated
(0 / 1000)
ADT corrected
(0 / 1000)
ADT corrected (clipped)
(0 / 1000)
Original – Corrected (clipped)
(0 / 50)
M = 0.5 HU, σ = 10.3 HU
M = 1.5 HU, σ = 1.4 HU

Thank You!

This presentation will soon be available at www.dkfz.de/ct.

Job opportunities through DKFZ’s international PhD or Postdoctoral Fellowship programs (www.dkfz.de), or directly through Marc Kachelriess (marc.kachelriess@dkfz.de).

Parts of the reconstruction software were provided by RayConStruct® GmbH, Nürnberg, Germany.